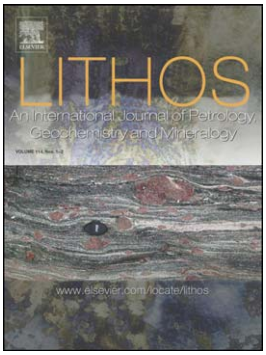

Origin of Permian OIB-like basalts in NW Thailand and implication on the Paleotethyan Ocean

Yuejun Wang, Huiying He, Yuzhi Zhang, Boontarika Srithai, Qinglai Feng, Peter A Cawood, Weiming Fan

PII: S0024-4937(16)30456-X
DOI: doi:10.1016/j.lithos.2016.12.021
Reference: LITHOS 4182

To appear in: *LITHOS*

Received date: 2 February 2016
Accepted date: 21 December 2016

Please cite this article as: Wang, Yuejun, He, Huiying, Zhang, Yuzhi, Srithai, Boontarika, Feng, Qinglai, Cawood, Peter A, Fan, Weiming, Origin of Permian OIB-like basalts in NW Thailand and implication on the Paleotethyan Ocean, *LITHOS* (2016), doi:10.1016/j.lithos.2016.12.021

Origin of Permian OIB-like basalts in NW Thailand and implication on the Paleotethyan Ocean

Yuejun Wang [1, 2, 3, *], Huiying He [1, 2], Yuzhi Zhang [1, 2],
Boontarika Srithai [4], Qinglai Feng [5] Peter A Cawood [6] Weiming Fan [3]

1 School of Earth Science and Geological Engineering, Sun Yat-sen University, Guangzhou 510275, China
2 Guangdong Key Laboratory of Geodynamics and Geohazards, Guangzhou 510275, China
3 CAS Center for Excellence in Tibetan Plateau Earth Sciences, Beijing 100101, China
4 Department of Geological Sciences, Faculty of Science, Chiang Mai University, Chiang Mai 50200, Thailand
5 State Key Laboratory of Geological Processes and Mineral Resources, Faculty of Earth Sciences, China University of Geosciences, Wuhan, 430074, China
6 Department of Earth Sciences, University of St Andrews, North Street, St Andrews KY169AL, UK

* Corresponding author
School of Earth Science and Geological Engineering
Sun Yat-sen University
No. 135, Xingang Xi Road, Guangzhou, 510275
People's Republic of China
Tel: 86-20-84111209
Email: wangyuejun@mail.sysu.edu.cn

Abstract

The basaltic rocks in NW Thailand belong to part of giant Southeast Asian igneous zone that delineates the extension of the Paleotethyan Ocean from SW China into NW Thailand. The Chiang Mai basaltic samples from the Chiang Dao, Fang, Lamphun and Ban Sahakorn sections are divisible into two groups of high-iron basalt. Group 1 has SiO_2 of 38.30-49.18 wt. %, FeOt of 13.09-25.37 wt.%, MgO of 8.38-1.60 wt.%, TiO_2 of 3.92-6.30 wt.%, which is rarely observed in nature. Group 2 shows SiO_2=44.71-49.21 wt. %, FeOt=10.88-14.34 wt. %, MgO= 5.24-16.11 wt.%, TiO_2= 2.22-3.07 wt.% and $mg^{\#}$=44-70. Olivine and pyroxene are responsible for the fractionation of the Group 2 magma whereas low oxygen fugacity during the late-stage differentiation of the Group 1 magma prolonged fractionation of ilmenite and magnetite. The onset of ilmenite and magnetite fractionations controls the distinct differentiation commencing at MgO = ~7 wt.%. Both groups show similar REE and primitive mantle-normalized patterns with insignificant Eu, Nb-Ta and Zr-Hf anomalies. They have similar Nd isotopic compositions with $\varepsilon_{Nd}(t)$ values ranging from +2.8 to +3.7 and similar Nb/La, Nb/U, Th/La, Zr/Nb, Th/Ta, La/Yb, Nb/Th, Nb/Y and Zr/Y, resembling those of OIB-like rocks. The representative basaltic sample yields the argon plateau age of 282.3 ± 1.4 Ma, suggestive of early Permian origin. Our data argue for Group 1 and Group 2 are coeval in the intra-oceanic seamount setting within the Paleotethyan Ocean, which at least continued till 283 Ma. These data, along with other observations, suggest that the Inthanon zone defines the main Paleotethyan suture zone, which northerly links

with the Changning-Menglian zone in SW China.

Keywords Early Permian; magma differentiation trend; OIB-like seamount basalt; Paleotethyan Ocean; NW Thailand

1. Introduction

The Paleotethys is the ocean basin that lay off northern Gondwana and its consumption resulted in the transfer and accretion of crustal blocks from Gondwana to the cratons of Asia (e.g., Sengör, 1984; Sone and Metcalfe, 2008; Metcalfe, 1996, 2006, 2013). Remnants of the oceanic track extend from the Alps through the Middle East to SW China and Peninsular Malaysia in SE Asia (e.g., Bullard et al., 1965; Acharyya, 1998; Metcalfe, 1998, 2002, 2006, 2013). The eastern Paleotethys, which runs from Nepal-India and South Tibet through SW Yunnan and NW Thailand to Malay Peninsula (Fig. 1a), records subduction leading to collision of the South Qiangtang/Sibumasu with North Qiangtang/Indochina/South China blocks (e.g., Hodges, 2000; Yin and Harrison, 2000; Searle et al., 2011; Sone and Metcalfe, 2008; Metcalfe, 1996, 2006, 2013). In Tibet and SW Yunnan, the Longmucuo-Shuanghu and Changning-Menglian suture zones mark the remnants of the eastern Paleotethyan Ocean (e.g., Zhong, 1998; Li et al., 2005; Feng et al., 2002, 2004, 2008; Wang et al., 2010; Fan et al., 2015). However, the southward extension of the Paleotethyan ocean in NW Thailand is not well defined, and the Mae Yuam Fault, the Chiang Rai Fault and Nan suture zone have all been proposed as ocean remnant in the region (Fig. 1b; e.g., Caridroit, 1993; Feng et al., 2002, 2004, 2008; Bunopas, 1994; Hada et al., 1997;

Mantajit, 1999; Barr and MacDonald, 1991; Ueno, 1999, 2003; Ferrari et al., 2008; Hara et al., 2009; Yang wt al., 2016).

In NW Thailand, mafic volcanic rocks are preserved in the following four belts from west to east: Chiang Rai-Chiang Mai, Chiang Khong-Tak, Phaisali-Chanthaburi and Loei-Phetchabun-Phai Sali belts (Fig. 2a). The mafic rocks could provide important information for constraining the mantle source and probing the tectonic setting. However, so far only limited study has been conducted in this field. The Chiang Mai-Chiang Rai volcanic belt lies within the Inthanon zone of NW Thailand, which is considered to be part of a giant igneous belt linking the Changning-Menglian volcanic zone to the north (SW Yunnan), and the Bentong-Raub zone to the south (Malay Peninsula), as shown in Figs. 1-2 (e.g., Sone and Metcalfe, 2008; Metcalfe, 1996, 1998, 2002, 2006, 2013; Barr et al., 2000; Wang et al., 2010). Abundant basaltic rocks in the belt are preserved and thus can provide important constraints on the tectonic evolution of the eastern Paleotethyan Ocean.

The general lithofacies and lithochemistry of the Chiang Rai-Chiang Mai volcanic belt have been illustrated by Baum and Hahn (1977), Hess and Koch (1979), Macdonald and Barr (1978), Barr et al. (1990) and Panjasawatwong (1999). However, no consensus has been reached on the nature of the rock association within the belt, which has been variously described as basic volcanic rocks with intermediate tufferous interlayer, "uncertain ophiolite" or pillow basalt (e.g., Hutchison, 1975, 1989; Baum and Hahn 1977; Ridd et al., 2011). The eruption timing for these rocks remains unresolved (Carboniferous vs. Permian vs. Permo-Triassic). Their tectonic setting

including subduction, within-plate, ocean and back-arc basin has been proposed (e.g., Bunopas et al., 1981, 1994; Hutchison, 1989; Barr et al., 1990; Caridroit, 1993; Panjasawatwong et al., 1995; Panjasawatwong, 1999; Ueno 1999, 2003; Charusiri et al., 2002; Metcalfe, 2002, 2013; Phajuy et al., 2005). These uncertainties existing in age, petrogenesis and tectonic setting are mainly due to the lack of detailed geochronological and geochemical data.

In this paper, a set of new geochronological, elemental and Sr-Nd isotopic data are presented for thirty-six basaltic samples, from the Chiang Dao, Fang, Lamphun and Ban Sahakorn volcanic profiles at the Chiang Mai-Chiang Rai area in NW Thailand (Fig. 2b). According to our study, our basaltic rocks are early Permian in age and different differentiation trends are showed. They have an OIB-like geochemical affinity, which indicates a within-plate seamount setting of the NW Thailand Paleotethyan Ocean.

2. Geological background

NW Thailand is bounded by the Bentong-Raub suture zone in Malaysia and the Changning-Menglian suture zone in SW China (Fig. 1a; e.g., Sone and Metcalfe, 2008; Metcalfe, 1998, 2006, 2013). From west to east, the region is divided into the Sibumasu block, the Inthanon and Sukhothai zones and the Indochina block, which are separated by the Mae Yuan Fault, the Chiang Rai Fault and the Nan suture zone (Figs. 1b and 2a-b； Barr and Macdonald, 1991).

The Sibumasu block lies between the Mogok metamorphic belt in Myanmar and

the Inthanon zone in NW Thailand. It extends southwards into western Malay Peninsula (Fig. 1a), and is believed to be a part of the peri-Gondwanan Cimmerian continent that lay along the northeastern margin from the late Carboniferous to early Permian (e.g., Sengör, 1984; Metcalfe, 1996, 1998, 2006, 2013; Barber and Crow, 2003; Sevastjanova et al., 2011). It is also considered to be equivalent as the South Qiangtang block in Tibet, and the Baoshan and Tengchong blocks in SW China.

To the east of the Chiang Rai Fault is a continental terrane, variously referred to as the Sukhothai zone (used herein), Sukhothai Arc, or Sukhothai fold belt (Figs. 1b and 2; e.g., Bunopas et al., 1981; Barr and Macdonald, 1991). It is separated from the Indochina block by the Nan suture zone (e.g., Ueno and Hisada, 2001; Panjasawatwong et al., 2003; Sone and Metcalfe, 2008; Qian et al., 2013, 2015; Yang et al., 2016). The zone consists of Paleozoic greywackes, shales, limestones and schists, and Carboniferous-Permian volcanoclastic rocks, radiolarian cherts and quartzites, along with small amount of granites (e.g., Fang et al., 1994; Ueno and Hisada, 2001; Sone and Metcalfe, 2008; Metcalfe, 2006, 2013; Ridd et al., 2011). In this zone, the pre-Mesozoic strata are uncomfortably overlain by the middle/upper Triassic molasse and Jurassic epicontinental sedimentary sequences.

The Indochina block is separated from the South China block by the Ailaoshan-Song Ma suture zone and from the Sukhothai zone by the Nan suture zone (e.g., Metcalfe, 1998, 2013; Morley, 2001; Lepvrier et al., 2008; Fan et al., 2010). In the block, the Proterozoic basement and Paleozoic-Triassic package are similar to those of the Yangtze block (e.g., Zhong, 1998; Peng et al., 2008, 2013; Wongwanich and

Boucot, 2011). Upper Mesozoic strata are characterized by a continental red bed package, such as that in the Khorat Plateau Basin (Ridd et al., 2011).

The Inthanon zone is bounded by the Mae Yuam and Chiang Rai faults and consists of a metamorphic assemblage exposed at Doi Inthanon and Doi Suthep, Cambro-Ordovician and Devonian limestones and sandstones, scattered Carboniferous-Permian carbonates, shales, sandstones and basalts, and upper Triassic-Jurassic volcanoclastic rocks, as well as Permo-Triassic granites and granodiorites (Fig. 2b-c; e.g., Feng et al., 2002, 2004, 2008; Ueno and Hisada, 2001; Wonganan et al., 2007; Hara et al., 2009; Ridd et al., 2011, 2015). It has been alternatively proposed as part of the Sibumasu block (e.g., Cobbing et al., 1992; Charusiri et al., 1993; Sone and Metcalfe, 2008; Metcalfe, 1996, 2002, 2013) or as a Paleotethyan suture zone separating the Sukhothai zone to the east from the Sibumasu block to the west (e.g., Ueno and Hisada, 2001; Hara et al., 2009).

Carboniferous–Permian limestones, sandstones, shales, and basaltic rocks (Fig. 2b; e.g., Ridd et al., 2011, 2015) characterize the Inthanon zone. The basaltic rocks defined the Chiang Rai–Chiang Mai volcanic zone and composed of basalts, basaltic andesites, hyaloclastites and pillow breccias (e.g., Bunopas et al., 1981, 1994; Chuaviroj et al., 1980; Phajuy et al., 2005; Ridd et al., 2011, 2015). They have previously been inferred to be uncomfortably underlain by the Carboniferous sedimentary rocks and overlain by Permian/Triassic limestones, cherts and shales. In addition, late Carboniferous to early Middle Permian fusulinid fragments occurred in the carbonate cement of the pillow breccias (e.g., Ridd et al., 2011). Thus, these

basaltic rocks have been assigned to be of Carboniferous, Carboniferous– Permian, Permian or Permian-Triassic origin (e.g., Macdonald and Barr, 1978; Barr et al., 1990; Panjasawatwong, 1999). In the Chiang Dao and Kae Noi areas, massive and vesicular basalts characterize the volcanic sequences and are overlain by tuffaceous limestones, and dolomites and dolomitic limestones of the Dan Lan Hoi Group (Fig. 2b-c, Feng et al., 2002, 2004). Bunopas (1981) and Chuaviroj et al. (1980) considered that the Dan Lan Hoi Group may be middle Permian to Triassic in age. Phajuy et al., (2005) argued that its origin could be between Late Carboniferous and early Middle Permian. The fossils with the indicator of the Carboniferous -early Triassic origin are also reported in the limestones in NW Thailand by Caridroitet al. (1993); Ueno (1999, 2003); Feng et al. (2004, 2008), Wonganan et al. (2005), Fontaine et al. (2005) and Miyahigashi et al.(2009).

In this study, samples were collected from four representative volcanic profiles at Chiang Dao (19°23'09.85"N, 98°55'37.54"E), southwwest of Fang (19° 38'03.71"N, 99°07'37.99"E), east of Ban Sahakorn (19°06'29.95"N, 99°27' 18.03"E) and east of Chiang Mai (18°49'45.29"N', 99°15'36.69"E), as shown in Figure 2b. Their mineral assemblage is mainly characterized by feldspar (30–60 % by volume), pyroxene (15–40 %), magnetite and ilmenite (1-16 %) and amphibole (~2 %), with minor amounts of biotite, zircon, titanite and apatite (Fig. 3a-d). Olivine (~5%) is also observed in several samples.

3. Analytical methods

Any altered surfaces on rock samples were removed prior to crushing to chips. Fresh chips were cleaned in an ultrasonic bath using de-ionized water. Chips from sample TG-4A were handpicked under a binocular microscope, and crushed to 40-60-mesh for $^{40}Ar/^{39}Ar$ analyses. Chips from other samples were crushed to 200-mesh in an agate mill for major oxide, trace element, and Sr-Nd isotopic analyses.

Laser $^{40}Ar/^{39}Ar$ step-heating measurements on sample TG-4A were carried out using the GV-5400 mass spectrometer at the Guangzhou Institute of Geochemistry (GIG), the Chinese Academy of Sciences (CAS). Sample and monitoring standard ZBH-2506 were irradiated at the 49-2 reactor for 54 h along with the biotite monitor ZBH-25 under the standard age of 132.7 ± 1.2 Ma. Correction factors for interfering argon isotopes derived from Ca and K involve $(^{39}Ar/^{37}Ar)_{Ca}$, $(^{36}Ar/^{37}Ar)_{Ca}$ and $(^{40}Ar/^{39}Ar)_{K}$ of 8.984×10^{-4}, 2.673×10^{-4} and 5.97×10^{-3}, respectively. The crusher consists of a 210 mm long, 28 mm bore diameter high temperature resistant stainless steel tube (Tmax~1200°C). The extraction and purification lines were baked out for ca. 10 h at 150 °C with heating tape and the crusher at 250 °C with an external tube furnace. The blanks are: ^{36}Ar (0.002-0.004) mV, ^{37}Ar (0.0002-0.0006) mV, ^{38}Ar (0.0004-0.0015) mV, ^{39}Ar (0.0025-0.0051) mV and ^{40}Ar (0.51-1.3) mV. The $^{40}Ar/^{39}Ar$ dating results and errors were calculated using the ArArCALC software (Koppers, 2002).

Major element oxides were analyzed at GIG, CAS using a Rigaku RIX 2000 X-ray fluorescence spectrometer on fused glass beads. The relative standard

derivations are kept within 5%, and totals are 100 ± 1 wt.%. Details of the procedures are described by Li et al. (2005). Trace element contents were performed at GIG, CAS by inductively coupled plasma mass spectrometry (ICP-MS). Approximately 100 mg samples were digested with 1 ml of HF and 0.5 ml HNO_3 in screw top PTFE-lined stainless steel bombs at 190 °C for 12 h. Insoluble residues are dissolved using 8 ml of 40 % HNO_3 (v/v) heated to 110 °C for 3 h. Its detailed analytical procedure is described by Wei et al. (2002). Sample powders for Sr and Nd isotopic analyses were spiked with mixed isotope tracers, dissolved in Teflon beakers with HF+HNO_3 acids, and separated by a conventional cation exchange technique and run on single Wand Ta–Re double filaments, respectively (Liang et al., 2003). Sr and Nd isotopic analyses were performed on a Micromass Isoprobe multi-collector ICPMS at the GIG, CAS. Total procedure blanks were in the range of 200-500 pg for Sr and ≤ 50 pg for Nd. $^{87}Rb/^{86}Sr$ and $^{147}Sm/^{144}Nd$ were calculated using the Rb, Sr, Sm and Nd contents measured by ICP-MS and the $^{87}Sr/^{86}Sr$ of the (NIST) SRM 987 standard and $^{143}Nd/^{144}Nd$ of the La Jolla standard are 0.710265 ± 12 (2σ) and 0.511862 ± 10 (2σ), respectively.

4. Analytical results

4.1 Whole-rock Ar-Ar geochronology

Sample TG-4A is taken from the site of 19° 38'03.71"N and 99°07'37.99"E (Fig. 2b). The analytical results and age spectra are in Supplementary Dataset 1 and Figure 4, respectively. The whole-rock grains give $^{40}Ar/^{39}Ar$ apparent age of 280.6–287.1 Ma

during the eighth to nineteen continuous heating steps and yield a plateau age of 282.3 ± 1.4 Ma with MSWD = 1.0. This plateau age is defined by > 80% of total ^{39}Ar released gas with invariability for a 2σ level of uncertainty. The corresponding normal and inverse isochron ages are 283.5 ± 2.7 Ma and 286.3 ± 2.8 Ma, respectively, consistent within error to the plateau age. The initial $^{40}Ar/^{36}Ar$ of 294.1 is similar to the present atmospheric $^{40}Ar/^{36}Ar$ (295.5), indicating that excess argon is insignificant. This suggests the plateau age of 284 Ma being reliable. Thus, it is inferred that the Chiang Dao basalt in NW Thailand erupted at early Permian period, also evidenced by the development of the early Permian fusulinids in the Chiang Dao stratigraphic sequence (e.g., Ratanasthien et al., 1999; Feng et al., 2002, 2004, 2008).

4.2 Geochemical results

Whole-rock major oxides, trace element, and Sr-Nd isotopic analyses are listed in Supplementary Dataset 2. Loss-on-ignition values for the 36 analyzed samples range from 0.98 to 5.18 wt.%. SiO_2 content ranges from 38.30 wt.% to 49.21 wt.% (volatile-free) and MgO content from 16.11 wt.% to 1.60 wt.%. Taking into account the mobility of alkaline elements, Zr/Ti and Nb/Y are selected for lithological classification. In Fig. 5a, these samples show an alkaline affinity and fall in the alkaline basalt field. However, these samples have variable FeOt and TiO_2 contents with values as high as 25.37 wt.% and 6.30 wt.%, respectively. On the SiO_2 vs FeOt and MgO vs TiO_2 diagrams (Fig. 5b-c), our samples plot along different magma evolved trends, which are herein referred to as Group 1 and Group 2 (e.g., Brooks et

al., 1991; Toplis and Carroll, 1995; Jang et al., 2001; Xu et al., 2003). Such distinct differentiation trends are also shown in the plots of MgO and other major oxides (Fig. 6a-f).

Group 1, represented by the 18 samples mainly from the Chiang Dao and Fang profiles (Fig. 2b-c), shows high FeOt (>13 wt%) and TiO_2 (>3.5wt%) contents (Fig. 5b-c) with SiO_2 ranging from 38.30 to 49.18 wt.%. FeOt linearly increases from 13.09 wt.% to 25.37 wt.% and TiO_2 from 3.92 wt.% to 6.30 wt.%, when MgO decreases from 8.38 wt.% to 1.60 wt.% (Supplementary Dataset w and Fig. 5b-c). The Group 1samples fall into the field of the proposed Fenner evolved trends of the Skaergaard intrusion and the Emeishan large igneous province (Fig. 5b-c; e.g., Brooks and Nielsen, 1978; Brooks et al., 1991; McBirney, 1996; Tegner, 1997; Jang et al., 2001; Xu et al., 2003; Thy, et al., 2006, 2009). They have Al_2O_3 ranging from 13.90 to 17.84 wt.%, K_2O+Na_2O from 3.74 to 6.97 wt.% and CaO from 1.16 to 8.58 wt.%. P_2O_5 and MnO are in the range of 0.12-1.40 wt.% and 0.07- 0.18 wt.%, respectively. On Harker diagrams (Fig. 6a-f), Al_2O_3, TiO_2, FeOt and K_2O+Na_2O increase whereas SiO_2, CaO and MnO decrease with decreasing MgO. The mg-number ranges from 12 to 50, Ni from 14 to 123 ppm, and Cr from 12 to 223 ppm, V from 257 to 584 ppm and Sc from 24.7 to 32.3 ppm, respectively (Supplementary Dataset 2 and Fig. 7a-e).

Group 2, consists of 18 samples mostly from the Ban Sahakorn and Chiang Mai profiles (Fig. 2b), and generally fall into the range of the Bowen evolution magma defined by the Skaergaard intrusion and the Emeishan large igneous

province (e.g., Brooks and Nielsen, 1978; Brooks et al., 1991; McBirney, 1996; Tegner, 1997; Jang et al., 2001; Xu et al., 2003; Thy, et al., 2006, 2009). The Group 2 samples have relatively lower FeOt (<14.5 wt%) and TiO_2 (<3.50 wt.%) contents than those of Group 1 samples (Fig. 5b-c). SiO_2 contents of the Group 2 samples range from 44.71 to 49.21 wt.%, MgO from 5.24 to 16.11 wt.%, Al_2O_3 from 8.73 to 15.29 wt.%, CaO from 7.95 to 12.94 wt.%, K_2O+Na_2O from 1.20 to 4.79 wt.%, and P_2O_5 from 0.13 to 0.41 wt.% (Supplementary Dataset 2 and Fig. 6a–f). They have higher mg-number (44-70), Ni (59-718 ppm), Cr (44-723 ppm) but lower Sc (18.5-29.6 ppm) and V (236-361 ppm) contents in comparison with those of the Group 1 samples (Fig. 7a-d). TiO_2, CaO, FeOt and MnO contents are slightly various irrespective of MgO but Al_2O_3 and K_2O+Na_2O increase and Co, Cr and Ni sharply decrease with decreasing MgO (Figs. 5d and 6-7). Group 2 shows distinct differentiation trends from Group 1 in Fig. 6a-f.

On plots of Zr vs immobile elements (e.g., Y, Nb, La and Th), both groups are positively correlated (Fig. 7f-i). However, Zr content does not show systematic correlation with mobile elements (e.g., Rb, Sr and K; Fig. 7j). Group 1 has higher incompatible element contents but identical Zr/La, Zr/Nb, Zr/Y and Zr/Th compared to those of Group 2 (Fig. 7f-i). In Figure 8a, both groups have similar chondrite-normalized REE pattern with high (La/Yb)cn (5.28-14.20), (Gd/Yb)cn (2.04-3.91) and insignificant europium anomalies (δEu=0.83-1.27), generally similar to those of ocean island basalts (OIB) in spite that Group 1 have higher contents of incompatible elements than Group 2. In Figure 8b, both groups generally lack Nb-Ta

and Zr-Hf anomalies, consistent with average OIB, with the exception of slightly positive Ti and negative Y anomalies.

Seven representative samples from Group 1 have $^{87}Sr/^{86}Sr$ of 0.70390- 0.72551 and $^{143}Nd/^{144}Nd$ of 0.512702-0.512721 with $^{147}Sm/^{144}Nd$ of 0.134- 0.149. The corresponding $^{87}Sr/^{86}Sr(i)$ range from 0.70382 to 0.70510 and $\varepsilon_{Nd}(t)$ values from +3.1 to +3.7, respectively. Seven samples from Group 2 give initial $^{87}Sr/^{86}Sr$ of 0.70355-0.70655 and $\varepsilon_{Nd}(t)$ values of +2.8~+3.7, respectively. Such Sr-Nd isotopic compositions are lower than those of Hawaii OIB but similar to those of Kenya, Samoa and Emeishan high-Ti basalts (Fig. 9).

5. Discussion

5.1 Magma differentiation

It is important to assess whether or not the samples underwent low-temperature alteration and crustal contamination before speculating on their mantle source (e.g., DePaolo, 1981). Our samples might have been subjected to various degrees of alteration viewed from high loss on ignition (0.98-5.18 wt%) and greenschist-facies metamorphism. However, the consistency of the dataset in the REE- and primitive mantle-normalized patterns in Fig. 8a–b, as well as the lack of correlation among MgO, Nb, La, Zr and Nd isotopic ratios and LOI preclude the significant effects of low-temperature alteration and metamorphic on the almost major element, REE and HFSE, along with and Nd isotopic ratios.

The Group 1 high-iron magma shows relatively constant Nd isotopic ratios

mg-number of 12-50, MgO of 1.60-8.38 wt.%. Such observations argue against the significant involvement of the crustal materials. It is usual that the crustal assimilation en route would sharply increase the oxygen fugacity of the magma (e.g., Xu et al., 2003), which contradicts the lower oxygen fugacity condition for generating high-iron magma (e.g., Sparks et al., 1980; Brooks et al., 1991; Toplis and Carroll, 1995; Xu et al., 2003). Group 2 has high mg-number (44-70) and MgO content (5.24-16.11 wt.%), contradict to what would be expected for crustal contamination (e.g. DePaolo, 1981). In addition, both groups have higher TiO_2 content and Ti/Y values than those of the bulk continental crust (Taylor and McLennan, 1995). They show TiO_2 of more than 1.70 wt.% and Nb/La from 0.99 to 1.31, and Zr/Nb from 6.5 to 9.6. Nb anomalies are insignificant (Fig. 8b). The synthesis of these observations suggests that high-iron basaltic magmas in Chiang Mai area of NW Thailand might have undergone poor crustal contamination during their ascent.

In plots of Ni vs Th, and Yb vs La/Yb and Tb/Yb (Fig. 10a-c), the Group 1 and 2 samples plot along the trends of fractionation crystallization rather than of partial melting or source heterogeneity. They give lower Th/Ta (1.1-2.1) than that of the primitive mantle (2.3), further suggesting a near closed-system fractional crystallization of the primary magma. For Group 2 samples, decreasing MgO and FeOt with increasing SiO_2 suggests olivine and pyroxene fractionation (Figs. 5c and 6b). The relations between MgO and CaO and Al_2O_3 indicate that the Group 2 magma also underwent clinopyroxene fractionation (Fig. 6). Such a differentiation process is further supported by the decreasing Ni, Cr, V and Co with decreasing MgO. The

constant P_2O_5 and TiO_2 contents argue against the significant fractionation of apatite and ilmenite and magnetite. For Group 1 samples, FeOt and TiO_2 contents increase with decreasing MgO, distinct from those in Group 2 (Fig. 5b-c). They contain small phenocrysts of ilmenite and magnetite, indicative of the high Fe-Ti contents impossibly resulting from ilmenite and magnetite accumulation (e.g., Brooks et al., 1991; Jang et al., 2001; Xu et al., 2003). In contrast, the high FeO and TiO2 contents for these samples should be representative of the melt phase which eventually became the basalt whole-rocks (e.g., Tegner, 1997; Jang et al., 2001; Thy, et al., 2006, 2009). Available data from the Skaergaard intrusion and Emeishan large igneous province show that high-iron magma usually crystallizes in a closed or nearly closed system (e.g., Brooks and Nielsen, 1978; Brooks et al., 1991; Xu et al., 2003). These data synthetically indicate the Group 1 and 2 magmas being coeval in a nearly closed system.

On Harker diagrams, the Group 1 and Group 2 samples join at MgO = ~6-8 % (Figs. 5-6). The compositional divergence for Group 1 and 2 at MgO values of ~6-8 % is likely controlled by the onset of ilmenite and magnetite fractionations (e.g., Synder et al., 1993). For the Group 1 magma, V/Sc increases from 9.8-13.6 at MgO=~6-8 % to 20.8 at MgO of 2.15 wt.%. However, the ratio for Group 2 is relatively constant (from 10.0 to 13.2) irrespective of MgO. Such a change for both groups is marked by increasing in TiO_2 and FeOt contents, reflective of the oxygen fugacity in the primary magma. Experimental data demonstrate that oxygen fugacity strongly influences the behavior of ilmenite and magnetite during the magma differentiation and oxygen

fugacity in strongly fractionated lavas will lower since ilmenite and magnetite fractionation decreases Fe^{3+} contents (e.g., Toplis and Carroll, 1995; Xu et al., 2003; Rutherford et al., 2006). Olivine and pyroxene are generally involved in the early-stage of magma fractionation Once MgO content in the residual magma is less than ~7 wt.%, the lowering oxygen fugacity will significantly delay the fractionation crystallization of ilmenite and magnetite (e.g., Osborn, 1959; Brooks et al., 1991; Toplis and Carroll, 1995; Jang et al., 2001). This process will result in the generation of the Group 1 magma that strongly rich in FeOt (~24%) and TiO_2 (~6%) (Fig. 5b-c), as observed in the Skaergaard intrusion and the proposed Emeishan high-Ti lavas (e.g., Wager, 1960; McBirney, 1996; Xu et al., 2003).

5.2 Origin of Permian OIB-like basalts in NW Thailand

The Group 1 and Group 2 samples show different fractionation trends (Figs. 5c-d and 6a-f). However, they have similar chondrite-normalized REE and primitive mantle-normalized incompatible element patterns with insignificant Eu, Nb-Ta and Zr-Hf anomalies (Fig. 8a-b). Such characteristics are identical to those of OIB. Both groups have similar Nd isotopic compositions with $\varepsilon_{Nd}(t)$ values ranging from +2.8 to +3.7 (Fig. 9). Their Nb/La ranges from 0.95 to 1.31, Nb/U from 25 to 56 and Th/La from 0.08 to 0.14, Zr/Nb from 5.7 to 9.6 and Th/Ta from 1.1 to 2.0. La/Yb, Ce/Pb, Th/Ta, Nb/Th, Nb/Y and Zr/Y all fall in or near the range for OIB, distinct from those of N-MORB and arc volcanics (Fig. 7f-j, 8a-b and 11a-d; e.g., Sun and McDonough, 1989). These signatures indicate a similar OIB-like origin for Group 1 and Group 2

when significant crustal contamination is precluded. On the Zr/Nb vs Ce/Y diagram (Deniel, 1998), both groups plot in a similar field indicating low degrees of melting of a garnet-bearing mantle source (Fig. 12a). The high La/Sm (2.75–4.12) and Sm/Yb (2.67–4.41) also argue for a low-degree melting product across the garnet–spinel lherzolite column (Fig. 12b; Lassiter and DePaolo, 1997).

In the rock archive, high-iron magma is comparatively rare (e.g. Leybourne et al., 1999). Two petrogenetic models are used to understand their origination involving (1) lherzolite with Fe-rich eclogite/pyroxenite blobs/streaks and (2) mantle wedge metasomatized by slab melt/delaminated refractory slab (Hauri, 1996; Takahasi et al., 1998; Kerrich et al., 1999; Leybourne et al., 1999; Gibson et al., 2000; Gibson, 2002; Wang et al., 2004, 2008). Our high-iron samples do not show the geochemical fingerprint of a subduction-modified mantle wedge. In addition, on the Chiang Dao profile in NW Thailand, the high-iron basalts are overlain by Permian shallow-marine carbonate (Zhang et al., 2016; Fig. 2c). Such phenomena resemble those in the Changning-Menglian suture zone in SW Yunnan that are interpreted to form in seamount setting (e.g., Feng et al., 2002, 2004, 2008). As mentioned above, our data in Figs. 6-9 suggest that the least fractionated samples have a composition of SiO_2 = ~45 wt.%, Al_2O_3 =~10 wt.%, FeO =~14 wt.%, MgO =~15 wt.%, CaO =~12 wt.%, K_2O+ Na_2O =~2 wt.% and TiO_2 =~2.5 wt.% (Figs. 5-6). The primary magma for both groups is Fe-, Mg- and Ti-rich and the source might be the garnet–spinel lherzolite with eclogite/pyroxenite streaks. Experimental studies indicate that ~50 % melting of eclogitic streaks can generate high-iron melt

with elevated Al_2O_3 content and Nb/La (e.g., Rapp et al., 1991; Gasparik and Litvin, 2002; Klemme et al., 2002; Gibson, 2002). Consequently, it is inferred for the Permian OIB-like Group 1 and Group 2 basalts in NW Thailand having originated from a similar source consisting of garnet–spinel lherzolite with eclogitic or pyroxenite streaks in spite of the distinct magma differentiation trends.

5.3 Tectonic implications

Our results above show that the Group 1 and Group 2 basaltic rocks in NW Thailand have an OIB-like geochemical affinity. On a variety of plots involving immobile elements, they fall into the intra-plate or seamount basalt field (Fig. 11c-d). These samples display low Zr/Y, Nb/Y, La/Yb, Th/Yb and Nb/Yb, distinct from the field of N-MORB. In Figure 11a-b, they plot along the MORB–OIB array near to OIB. Such signatures suggest an intraplate continental rift or oceanic setting (e.g., Lutkov, 1991; Volkova and Budanov, 1999; Gao and Klemd, 2003).

High-iron magma is occasionally observed in continental rift and mantle plume settings, along with divergent plate margin setting with thin crust (e.g., mid-oceanic ridge, Hunter and Sparks, 1987; Brook et al., 1991; Gibson, 2002; Harper, 2003; Higgins, 2005; Veksler et al., 2006; Namur et al., 2010). Our sample from the Chiang Dao profile yields an Ar-Ar age of 283 Ma. Such age, along with the early Permian fusulinids in the Chiang Dao stratigraphic sequence (Ratanasthien et al., 1999; Feng et al., 2002, 2004), indicating an early Permian eruption. In addition, Carboniferous -early Permian fusulinid fossil, foraminifers, minor corals and conodont are identified

in the limestones underlain by the massive basalt from the Mae Tha and Ban Pha Daeng areas in NW Thailand (Ratanasthien et al., 1999; Ueno, 1999, 2003; Fontaine et al., 2005). Such observations indicate the volcanic rocks in Chiang Mai area erupted at Carboniferous-early Permian. During this time, available geological data in NW Thailand do not reveal the presence of the large-scale doming, or dike swarms and anorogenic igneous activity, and thus against the plume setting. In addition, the magma differentiation trends revealed by our samples are uncommon in continental environments since crustal contamination in continental flood basalts might result in increases in oxygen fugacity of the magma (Xu et al., 2003), further precluding the possibility of a continental large igneous province setting for the Group 1 and Group 2 magma. In contrast, late Paleozoic ocean remnants consisting of basalts, pelagic radiolarian cherts and limestones, mudstones and turbidites are widespread in this area (Caridroit, 1993; Fang et al., 1994; Feng et al., 2002, 2004, 2008; Wonganan and Caridroit, 2005; Wakita and Metcalfe, 2005; Ridd et al., 2011). Devonian to Middle Triassic deep marine radiolarian cherts are well preserved in isolated sheets along the Chiang Rai-Mae Sariang area in the Inthanon zone (e.g., Chonglakmani, 2001; Feng et al., 2002, 2004; Wakita and Metcalfe, 2005; Radon et al., 2006; Sone and Metcalfe, 2008; Ridd et al., 2011). These signatures, along with late Paleozoic fauna in the area, indicate the presence of a long-lived ocean basin in NW Thailand (e.g.,Caridroitet al., 1993; Feng et al., 2004, 2008; Wonganan et al., 2005). Wakita and Metcalfe (2005) reported an ocean-floor stratigraphy ranging from pillow basalt up through radiolarian chert, interbedded radiolarian chert and pelagic limestones to deep sea argillites

nearby the Chiang Mai city. Thus Group 1 and Group 2 occur in a Paleotethyan oceanic intra-plate setting.

On the plot of Th/Yb vs (La/Sm)cn (Fig. 11d), the samples overlap with the seamounts at the East Pacific Rise, Permian seamount-like blueschist in SW Yunnan, and the Daimao seamount in the South China Sea (e.g., Pearce, 2008; John et al., 2010; Fan et al., 2015; Yan et al., 2015). Our field investigations indicate that the Group 1 and Group 2 basalts are overlain by Carboniferous-early Permian shallow-marine carbonates devoid of any continental detrital input, with the Doi Chiang Dao, Fang and Kae Noi profiles resembling typical seamount stratigraphic successions (Fig. 2c; Ratanasthien et al., 1999; Gradstein et al., 2004; Feng et al., 2002, 2004, 2008). Ueno (1999, 2003) and Feng et al. (2002, 2004, 2008) concluded that long and continuous carbonate deposition lacking any siliciclastic input is distinct from the normal shelf carbonates and can only be accomplished in the isolated intra-oceanic setting, e.g., seamount or oceanic plateau (Metcalfe, 2002, 2013; Wakita and Metcalfe, 2005; Feng et al., 2002, 2008; Ueno, 1999, 2003). As a result, the OIB-type Group 1 and Group 2 rocks most likely represent the basaltic substrate of a seamount–capped by shallow-marine carbonate build-ups in the intra-oceanic setting. Taking into account the spatial distribution of our Permian seamount basalts, which are mainly exposed within the Inthanon zone between the Mae Yuam and Chiang Rai faults, it is concluded that the Inthanon zone constitutes the remnants of the Paleotethyan ocean in NW Thailand (e.g., Barr and Macdonald, 1991).

It has been a matter of debate as to whether the Paleotethyan main suture in

NW Thailand lay along the Inthanon zone, Nan zone or Mae Yuam fault (e.g., Metcalfe, 1998, 2002, 2010, 2013; Sone and Metcalfe, 2008; Ueno and Tsutsumi, 2009). In NW Thailand, the Sukhothai zone and the Indochina block lie to the east of the Chang Rai Fault, and are separated by the Nan suture zone (Fig. 2a-b； Barr and Macdonald, 1991). Available geological data show that the Nan suture zone represents the Carboniferous-early Triassic back-arc basin that links northward with the time equivalent Jinhong and/or Ailaoshan back-arc basins (e.g., Metcalfe, 1998, 2002, 2013; Panjasawatwong et al., 2003; Lepvrier et al., 2008; Sone and Metcalfe, 2008; Fan et al., 2010, 2015; Oliver et al., 2014; Qian et al., 2013, 2015). The synthesis of these data suggests a Permian-Triassic supra-subduction zone with a northward (eastward in the present configuration) subduction polarity. The spatial pattern of the trench-arc system is shown in Fig. 13, from west to east, which is characterized by the Sibumasu block, Inthanon zone, Sukhothai zone, Nan back-arc zone and Indochina block, respectively. The Paleotethyan oceanic crust in NW Thailand is older than 283 Ma for the seamount to be built. The Inthanon zone defines the Paleotethyan main suture zone with the Chiang Rai Fault for the eastern boundary in NW Thailand.

Acknowledgements

We would like to express our gratitude to Dr. T-P Peng, X-P Xia, L-Y Ma and X Qian for their help during fieldwork, geochemical and mineral Ar-Ar analyses. We also thank Profs. D-C Zhu and K-N Pang for their thorough, critical and constructive

reviews and comments, and S-L Chuang for his helpful editorial suggestion. Financial supports from National Science Foundation of China (41190073, 41372198 and 40490613), National Basic Research Program of China (2014CB440901 and 2016YFC0600303) and “the Fundamental Research Funds for the Central Universities to SYSU" are gratefully acknowledged.

References

Acharyya, S.K., 1998. Break-up of the Greater Indo-Australian Continent and accretion of blocks framing South and East Asia. Journal of Geodynamics 26 (1), 149–170.

Barber, A.J., Crow, M.J., 2003. An evaluation of plate tectonic models for the development of Sumatra. Gondwana Research 6, 1–28.

Barr S.M., Macdonald A.S., 1991. Toward a Late Paleozoic-Early Mesozoic tectonic model for Thailand. Journal of Thailand Geosciences 1, 11–22.

Barr, S.M., Macdonald, A.S., Dunning, D.R., Ounchanum, P., Yaowanoiyothin, W., 2000. U-Pb zircon age, and Paleotectonic setting of the Lampang volcanic belt, Northern Thailand. Journal of Geology Society, London 157, 553–563.

Barr, S.M., Tantisukrit, C., Yaowanoiyothin, W., Macdonald, A.S., 1990. Petrology and tectonic implications of Upper Palaeozoic volcanic rocks of the Chiang Mai belt, northern Thailand. Journal of Southeast Asian Earth Sciences 4, 37–47.

Bowen, N. L., 1928. The evolution of the igneous rocks. Princeton: Princeton University Press 1–334.

Brooks, C.K., Nielson, T.F.D., 1978. Early stages in the differentiation of the Skaergaard magmas

as revealed by a closed related suite of dike rocks. Lithos 11, 1–14.

Bullard, E.C., Everett, J.E., Smith, A.G., 1965. The fit of the continents around the Atlantic: a symposium on continental drift. Philosophical Transactions of the Royal Society of London. Series A 258, 41–51.

Bunopas S. 1994. The regional stratigraphy, paleogeographic and tectonic events of Thailand and continental Southeast Asia. In: Angsuwathana P, Wongwanich T, Tansathien W, et al, eds. Proceedings of the International Symposium on Stratigraphic Correlation of Southeast Asia. Department of Mineral Resources of Thailand and Thai Working Group of IGCP 306. Bangkok, Thailand 2–24.

Bunopas, S., 1981. Paleogeographic history of western Thailand and adjacent parts of Southeast Asia: A plate tectonic interpretation, Geological Survey of Thailand, Special Paper 5. Department of Mineral Resources of Thailand, Bangkok p. 810.

Caridroit M, Bohlke D, Lamchuan A, et al. 1993. A mixed Radiolarian fauna (Permian/Triassic) from clastics of the Mae Sariang area, northwestern Thailand. In: Thanasuthipitak T, ed. Proceedings of the International Symposium on Biostratigraphy of Mainland Southeast Asia. Facies and Paleontology. Chiang Mai. 2, 401—413.

Caridroit, M., 1993. Permian radiolaria from NW Thailand. In: Thana-Suthipitak. T. (ed.) Proceedings of the international symposium on biostratigraphy of Mainland Southeast Asia Facies and Paleontology 1, Chiang Mai, Thailand 83–96.

Charusiri, P., Clark, H.A., Farrar, E., Archibald, D., Charusiri, B., 1993. Granite belts in Thailand: Evidence from the $^{40}Ar/^{39}Ar$ geochronological and geological syntheses. Journal of Southeast Asian Earth Sciences 8, 127–136.

Charusiri, P., Daorerk, V., Archibald, D., 2002. Geotectonic evolution of Thailand: A new synthesis. Journal of the Geological Society of Thailand 1, 1–20.

Chonglakmani, C., Feng, Q.L., Ingavat-Helmcke, R., Helmcke, D., 2001. Correlation of Tectono-stratigraphic units in Northern Thailand with those of Western Yunnan (China). Earth Science 12, 207–213.

Cobbing, E.J., Pitfield, P.E., Darbyshire, D.P.F., Mallick, D.I.J., 1992. The granites of the South-East Asian tin belt. Overseas Memoir of the British Geological Survey 10, 1–369 Her Majesty's Sth Off, Norfolk, England.

Deniel, C., 1998. Geochemical and isotopic (Sr, Nd, Pb) evidence for plume–lithosphere interactions in the genesis of Grande Comore magmas (Indian Ocean). Chemical Geology 144, 281–303.

DePaolo, D.J., 1981. Trace element and isotopic effects of combined wallrock assimilation and fractional crystallization. Earth and Planetary Science Letters 53, 189–202.

Fan, W.M., Wang, Y.J., Zhang, A.M., Zhang, F.F., Zhang, Y.Z., 2010. Permian arc-back-arc basin development along the Ailaoshan tectonic zone: Geochemical, isotopic and geochronological evidences from the Mojiang volcanic rocks, SW China. Lithos 119(3–4), 553–568.

Fan, W.M., Wang, Y.J., Zhang, Y.H., Zhang, Y.Z., Jourdan, F., Zi, J.W., Liu, H.C., 2015. Paleotethyan subduction process revealed from Triassic blueschists in the Lancang tectonic belt of Southwest China. Tectonophysics 662, 95–108.

Fang, N.Q., Liu, B.P., Feng, Q.L., 1994. Late Paleozoic and Triassic deep-water deposits and tectonic evolution of the Palaeotethys in the Changning-Menglian and Lancangjiang belts,

southwestern Yunnan. Journal of Southeast Asian Earth Sciences 9(4), 363–374.

Feng, Q.L., 2002. Stratigraphy of volcanic rocks in the Changning-Menglian belt in southwestern Yunnan, China. Journal of Asian Earth Sciences 20(6), 657–664.

Feng, Q.L., Chongpan, C., Dietrich, H., Ingavat-Helmcke, R., 2004. Long-lived Paleotethyan pelagic remnant inside Shan-Thai Block: Evidence from radiolarian biostratigraphy. Science in China Series D: Earth Sciences 47(12), 1113–1119.

Feng, Q.L., Yang, W.Q., Shen, S.Y., Chonglakmani, C., Malila, K., 2008. The Permian seamount stratigraphic sequence in Chiang Mai, North Thailand and its tectogeographic significance. Science in China Series D: Earth Sciences 51(2), 1768–1775.

Fenner, C. N., 1929. The crystallisation of basalt. American Journal of Science 18, 223–253.

Ferrari, O.M., Hochard, C., Stampfli, G.M., 2008. An alternative plate tectonic model for the Paleozoic–Early Mesozoic Paleotethyan evolution of Southeast Asia (Northern Thailand–Burma). Tectonophysics 451, 346–365.

Fontaine , H., Salyapongse, S., Tian, P., 2005. Chapter Ⅲ. An overview of the Carboniferous of Thailand with new data on the Carboniferous of Northeast and Northwest Thailand. In: Fontaine , H., Salyapongse, S., Suteethorn V., Tian, P., and Vachard, D., (eds) Sedimentary rocks of the Loei region, Northeast Thailand: stratigraphy, paleontology, sedimentology. Bureau of Geological Survey, Department of Mineral Resource, Bangkok 33–89.

Gao, J., Klemd, R., 2003. Formation of HP–LT rocks and their tectonic implications in the western Tianshan Orogen, NW China: Geochemical and age constraints. Lithos 66, 1–22.

Gasparik, T., Litvin, Y.A., 2002. Experimental investigation of the effect of metasomatism by carbonatic melt on the composition and structure of the deep mantle. Lithos 60, 129–143.

Gibson, S.A., 2002. Major element heterogeneity in Archean to Recent mantle plume starting-heads. Earth and Planetary Science Letters 195, 59–74.

Gibson, S.A., Thompson, R.N., Dickin, A.P., 2000. Ferropicrites: Geochemical evidence for Fe-rich streaks in upwelling mantle plumes. Earth and Planetary Science Letters 174, 355–374.

Gradstein, F., Ogg, J., Smith, A., 2004. A geologic time scale. Cambridge University Press, Cambridge.

Hada S, Bunopas S, Ishii K, Yoshikura S., 1997. Rift-drift history and the amalgamation of Shan-Thai and Indochina/East Malaya Blocks. In: Dheeradilok P, Hinthong C, Chaodumrong P, Putthapiban P., Tansathien W., Utha-Aroon C., Sattyarak N., Nuchanong T., and Techawan S., eds. Proceedings of the International Conference on Stratigraphy and Tectonic Evolution of Southeast Asia and the South Pacific. Bangkok, Thailand 273–286.

Hara, H., Wakita, K., Ueno, K., Kamata, Y., Hisada, K.I., Charusiri, P., Charoentitirat, T., Chaodumrong, P., 2009. Nature of accretion related to Paleo-Tethys subduction recorded in northern Thailand: constraints from mélange kinematics and illite crystallinity. Gondwana Research 16, 310–320.

Harper, G.D., 2003. Fe–Ti basalts and propagating-rift tectonics in the Josephine Ophiolite. Geological Society of America Bulletin 115, 771–787.

Hart, S.R., 1984. A large-scale isotope anomaly in the Southern Hemisphere mantle. Nature 309, 753–757.

Hauri, E.H., 1996. Major-element variability in the Hawaiian mantle plume. Nature 382, 415–419.

Hennig, D., Lehmann, B., Frei, D., Belyatsky, B., Zhao, X.F., Cabral, A.R., Zeng, P.S., Zhou, M.F.,

Schmidt, K., 2009. Early Permian seafloor to continental arc magmatism in the eastern Paleo-Tethys: U-Pb age and Nd-Sr isotope data from the southern Lancangjiang zone, Yunnan, China. Lithos 113 (3–4), 408–422.

Higgins, M.D., 2005. A new interpretation of the structure of the Sept Iles Intrusive suite, Canada. Lithos 83, 199–213.

Hodges, K.V., 2000. Tectonics of the Himalaya and southern Tibet from two perspectives. Geological Society of America Bulletin 112, 324–350.

Hunter, R.H., Sparks, R.S.J., 1987. The differentiation of the Skaergaard intrusion. Contributions to Mineralogy and Petrology 95, 451–461.

Hutchison, C.S., 1975. Ophiolites in Southeast Asia. Geological Society of America Bulletin 86, 797–806.

Hutchison, C.S., 1989. Geological evolution of South-East Asia. Oxford Monographs on Geology and Geophysics, vol. 13. Clarendon Press, Oxford, UK p. 368.

Jang, Y. D., Naslund, H. R., McBirney, A. R., 2001. The differentiation trend of the Skaergaard intrusion and the timing of magnetite crystallisation: Iron enrichment revisited. Earth and Planetary Science Letters 189, 189–196.

John, T., Scherer, E.E., Schenk, V., Herms, P., Halama, R., Garbe-Schönberg, D., 2010. Subducted seamounts in an eclogite-facies ophiolite sequence: the Andean Raspas Complex, SW Ecuador. Contributions to Mineralogy and Petrology 159, 265–284.

Kerrich, R., Polat, A., Wyman, D., Hollings, P., 1999. Trace element systematics of Mg- to Fe-tholeiitic basalt suites of the Superior Province: Implications for Archean mantle reservoirs and greenstone belt genesis. Lithos 46, 163–187.

Klemme, S., Blundy, J.D., Wood, B.J., 2002. Experimental constraints on major and trace element partitioning during partial melting of eclogite. Geochimica et Cosmochimica Acta 66, 3109–3123.

Konishi K. 1953. New Boultonia and other microfossils from north Thailand (Siam). Trans Proc Palaeont Soc Japan, N S, 12, 103—110.

Koppers, A.A.P., 2002. ArArCALC-software for $^{40}Ar/^{39}Ar$ age calculations. Computers and Geosciences 28, 605–619.

Lassiter J.C., Depaolo, D.J., 1997. Plume/lithosphere interaction in the generation of continental and oceanic flood basalts: Chemical and isotopic constraints. In: Mahoney, J.J., Coffin, M.F., (eds.). Geophysical Monograph. Washington, D.C., American Geophysical Union 100, 335–355.

Lepvrier, C., Van Vuong, N., Maluski, H., Truong Thi, P., Van Vu, T., 2008. Indosinian tectonics in Vietnam. Comptes Rendus Geoscience 340, 94–111.

Leybourne, M.I., Van Wagoner, N., Ayres, L.D., 1999. Partial melting of a refractory subducted slab in a Paleoproterozoic island arc: implications for global chemical cycles. Geology 27, 731–734.

Li, C., Zhai, Q.G., Xu, F., Zhu, Z.Y., 2005a. Kinematics of the active North-South-trending Chazang Co-Xainza tectonic Belt, Xizang (Tibet). Geological Review 51(4), 353–359 (in Chinese with English abstract).

Li, X.H., Su, L., Chung, S.L., Li, Z.X., Liu, Y., Song, B., Liu, D.Y., 2005b. Formation of the Jinchuan ultramafic intrusion and the world's third largest Ni–Cu sulfide deposit: associated with the ~825 Ma south China mantle plume? Geochemistry Geophysics Geosystems 6,

Q11004.

Liang, X.R., Wei, G.J., Li, X.H., Liu, Y., 2003. Precise measurement of $^{143}Nd/^{144}Nd$ and Sm/Nd ratios using multiple-collectors inductively coupled plasma-mass spectrometer (MC-ICPMS). Geochimica 32, 91–96.

Lutkov, V.S., 1991. The Earth's crust model of blueschist belt on the basis of investigation data on xenoliths in alkali basalts _South Tianshan. Doklady Akademii Nauk SSSR Dokl. Akad. Nauk SSSR 318, 1439–1442.

Macdonald, A.S., Barr, S.W., 1978. Tectonic significance of Late Carboniferous volcanic arc in Northern Thailand. Proceedings of the third regional conference on geology and mineral resources of Southeast Asia, Bangkok, Thailand pp. 151–156.

McBirney, A. R., 1996. The Skaergaard Intrusion, Layered Intrusions (ed. Cawthorn, R. J.), Amsterdam: Elsevier Science 1996, 147–180.

Metcalfe, I., 1996. Gondwanaland dispersion, Asian accretion and evolution of eastern Tethys. Australian Journal of Earth Science 43(6), 605–623.

Metcalfe, I., 1998. Palaeozoic and Mesozoic geological evolution of the SE Asian region: multidisciplinary constraints and implications for biogeography. Biogeography and Geological Evolution of SE Asia pp. 25–41.

Metcalfe, I., 2002. Permian tectonic framework and palaeogeography of SE Asia. Journal of Asian Earth Sciences 20, 551–566.

Metcalfe, I., 2006. Palaeozoic and Mesozoic tectonic evolution and palaeogeography of East Asian crustal fragments: The Korean Peninsula in context. Gondwana Research 9, 24–46.

Metcalfe, I., 2013. Gondwana dispersion and Asian accretion: Tectonic and palaeogeographic

evolution of eastern Tethys. Journal of Asian Earth Sciences 66, 1–33.

Miyahigashi, A., 2009. Foraminiferal assemblages and their ages from Paleo-Tethyan seamount-type limestone distributed in the Chiang Dao area, northern Thailand. Unpublished BSc thesis, Department of Earth System Science. Fukuoka University, Fukuoka (in Japanese with English abstract).

Namur, O., Charlier, B., Toplis, M.J., Higgins, M.D., Liégeois, J.P., Auwera, J.V., 2010. Crystallization sequence and magma chamber processes in the ferro basaltic Sept Iles layered intrusion, Canada. Journal of Petrology 51, 1203–1236.

Oliver, G., Khin, Zaw, Meffre, S., Hoston, M., Manaka, T., 2014. U-Pb zircon geochronology of Early Permian to Late Triassic rocks from Singapore and Johor: A plate tectonic reinterpretation. Gondwana Research 26, 132–143.

Osborn, E. F., 1959. Role of oxygen pressure in the crystallisation and differentiation of basaltic magmas. American Journal of Science 257, 609–647.

Panjasawatwong, Y., 1999. Petrology and tectonic setting of eruption of basaltic rocks penetrated in well GTE-1, San Kam Phaeng geothermal field, Chiang Mai, northern Thailand. In: Ratanasthein, B., Rieb, S.L. (Eds.), Proceedings of the international symposium on shallow Tethys (ST) 5, Chiang Mai, Thailand, February 1999. Department of Geological Sciences, Chiang Mai University, pp. 242–264.

Panjasawatwong, Y., 2003. Tectonic Setting of the Permo-Triassic Chiang Khong volcanic rocks, Northern Thailand based on petrochemical characteristics. Gondwana Research 6, 743–755.

Panjasawatwong, Y., Kanpeng, K., Ruangvatanasirikul, K., 1995. Basalts in Li Basin, northern Thailand. In: Thanvarachorn, S., Hokjaroen, S., Youngme, W. (eds.) Proceedings of the

international conference on geology, geotechnology and mineral resource of Indochina. Khon Kaen, Thailand, Department of Geotechnology, Khon Kaen University, 225–234.

Pearce, J.A., 2008. Geochemical fingerprinting of oceanic basalts with applications to ophiolite classification and the search for Archean oceanic crust. Lithos 100, 14–48.

Peng, T.P., Wang, Y.J., Zhao, G.C., Fan, W.M., Peng, B.X., 2008. Arc-like volcanic rocks from the southern Lancangjiang zone, SW China: geochronological and geochemical constraints on their petrogenesis and tectonic implications. Lithos 102, 358–373.

Peng, T.P., Wilde, S.A., Wang, Y.J., Fan, W.M., Peng, B.X., 2013. Mid-Triassic felsic igneous rocks from the southern Lancangjiang Zone, SW China: Petrogenesis and implications for the evolution of Paleo-Tethys. Lithos 168–169, 15–32.

Phajuy, B., Panjasawatwong, Y., Osataporn, P., 2005. Preliminary geochemical study of volcanic rocks in the Pang Mayao area, Phrao, Chiang Mai, northern Thailand: Tectonic setting of formation. Journal of Asian Earth Sciences 24, 765–776.

Qian, X., Feng, Q., Chonglakmani, C., Monjai, D., 2013. Geochemical and geochronological constrains on the Chiang Khong volcanic rocks (northwestern Thailand) and its tectonic implications. Frontiers of Earth Science 7, 508–521.

Qian, X., Feng, Q.L., Wang, Y.J., Chonglakmani, C., Monjai, D., 2015. Geochronological and geochemical constraints on the mafic rocks along the Luang Prabang zone: Carboniferous back-arc setting in northwest Laos. Lithos in press, doi:10.1016/j.lithos.2015.07.019.

Radon, C., Wonganan, N., Caridoroit, M., Perret-Mirouse, M., Degardin, J., 2006. Upper Devonian–Lower Carboniferous conodonts from Chiang Dao cherts. Northern Thailand, Rivista Italiana Di Paleontlogia E Stratigraifa 112(2), 191–206.

Rapp, R.P., Watson, E.B., Miller, C.F., 1991. Partial melting of amphibolite/eclogites and the origin of Archean trondhjemites and tonalites. Precambrian Research 51, 1–25.

Ratanasthien, B., Singharajwarapan, S., Chonglakmani, C., 1999. Pre-Shallow Tethys 5 Symposium Excursion, Guide Book. Chiang Mae, Thailand 14.

Ridd, M.F., 2015. East flank of the Sibumasu block in NW Thailand and Myanmar and its possible northward continuation into Yunnan: a review and suggested tectono-stratigraphic interpretation. Journal of Asian Earth Sciences 104, 160–174.

Ridd, M.F., Barber, A.J., Crow, M.J., 2011. The geology of Thailand. Geological Society, London pp.615.

Rutherford, L., Barovich, K., Foden, M.H.J., 2006. Continental ca. 1.7–1.69 Ga Fe-rich metatholeiites in the Curnamona Province, Australia: a record of melting of a heterogeneous, subduction-modified lithospheric mantle. Australian Journal of Earth Sciences 53, 501–519.

Sengör, A.M.C., 1984. The Cimmeride orogenic system and the tectonics of Eurasia. Geological Society of America Special Papers 195, 1–74.

Sevastjanova, I., Clements, B., Hall, R., Belousova, E.A., Griffin, W.F., Pearson, N., 2011. Granitic magmatism, basement ages, and provenance indicators in the Malay Peninsula: insights from detrital zircon U–Pb and Hf-isotope data. Gondwana Research 19, 1024–1039.

Sone, M., Metcalfe, I., 2008. Parallel Tethyan sutures in mainland Southeast Asia: new insights for Palaeo-Tethys closure and implications for the Indosinian Orogeny. Comptes Rendus Geosciences 340, 166–179.

Sparks, R. S., Meyer, P., Sigursson, H., 1980. Density variation amongst mid-ocean ridge basalts:

implications for magma mixing and the scarcity of primitive lavas. Earth and Planetary Science Letters 46, 419–430.

Sun, S.S., McDonough, W.F., 1989. Chemical and isotopic systematics of oceanic basalts: implications for mantle composition and processes. In: Saunders, A.D., Norry, M.J. (Eds.), Geological Society London Special Publications 42, 313–345.

Synder, D., Carmichael, I. S. E., Wiebe, R. A., 1993. Experimental study of liquid evolution in an Fe-rich layered mafic intrusion: constraints of Fe-Ti oxide precipitation on the T-f_{O2} and T-ρ paths of tholeiitic magmas, Contributions to Mineralogy and Petrology 113, 73–86.

Takahasi, E., Nakajima, K., Wright, T.L., 1998. Origin of the Columbia River basalts: melting model of a heterogeneous plume head. Earth and Planetary Science Letters 162, 63–80.

Taylor, S.R., McLennan, S.M., 1985. The continental crust: Its composition and evolution. Oxford Press Blackwell 1–312.

Tegner, C., 1997. Iron in plagioclase as a monitor of the differentiation of the Skaergaard intrusion. Contrib Mineral Petrol. 128, 45-51.

Thy, P., Lesher, C.E., Tegner, C., 2009. The Skaergaard liquid line of descent revisited. Contrib Mineral Petrol. 157, 735–747.

Thy, P., Lesher, C.E., Nielsen, T.F.D., Brooks, C.K., 2006. Experimental constraints on the Skaergaard liquid line of descent. Lithos 92, 154-180

Toplis, M. J., Carroll, M. R., 1995. An experimental study of the influence of oxygen fugacity on Fe-Ti oxide stability, phase relations, and mineral-melt equilibria in ferro-basaltic systems. Journal of Petrology 36, 1137–1170.

Toriyama R. 1944. On some Fusulinids from Northern Thai. Jap J Geol Geogr 19(1-4), 243—248.

Ueno K., Hisada K., 2001. The Nan-Uttaradit-Sa Kaeo suture as a main paleotethyan suture in Thailand: is it real? Gondwana Research 4(4), 804–806.

Ueno, K., 1999. Gondwana/Tethys divide in East Asia: Solution from Late Paleozoic foraminiferal paleobiogeography. In: Ratanasthien, B., and Ritb, S.L. (eds) Proceedings of the International on Shallow Tethys (ST) 5. Chiang Mai, 1–5 February 45–54.

Ueno, K., 2003. The Permian fusulinoidean faunas of the Sibumasu and Baoshan blocks: their implications for the paleogeographic and paleoclimatologic reconstruction of the Cimmerian Continent. Palaeogeography Palaeoclimatology Palaeoecology 193(1), 1–24.

Ueno, K., Tsutsumi, S., 2009. Lopingian (Late Permian) foraminiferal faunal succession of a Paleo-Tethyan mid-oceanic carbonate buildup: Shifodong Formation in the Changning-Menglian Belt, West Yunnan, Southwest China. Island Arc 18, 69–93.

Veksler, I.V., Dorfman, A.M., Danyushevsky, L.V., Jakobsen, j.k., Dingwell, D.B., 2006. Immiscible silicate liquid partition coefficients: implications for crystal-melt element partitioning and basalt petrogenesis. Contributions to Mineralogy and Petrology 152, 685–702.

Volkova, N.I., Budanov, V.I., 1999. Geochemical discrimination of metabasalt rocks of the Fan-Karategin transitional blueschist/greenschist belt, South Tianshan, Tajikistan; seamount volcanism and accretionary tectonics. Lithos 47(3–4), 201–216.

Wager, L. R., 1960. The major element variation of the Layered Series of the Skaergaard intrusion and a re-estimation of the average composition of the hidden layered series and of the successive residual magma, Journal of Petrology 1(1), 364–398.

Wakita, K., Metcalfe, I., 2005. Ocean plate stratigraphy in East and Southeast Asia. Journal of

Asian Earth Sciences 24, 679–702.

Wang, Y.J., Fan, W.M., Zhang, Y.H., Guo, F., Zhang, H.F., Peng, T.P., 2004. Geochemical, $^{40}Ar/^{39}Ar$ geochronological and Sr–Nd isotopic constraints on the origin of Paleoproterozoic mafic dikes from the southern Taihang Mountains and implications for the 1800 Ma event of the North China Craton. Precambrian Research 135, 55–79.

Wang, Y.J., Zhang, A.M., Fan,W.M., Peng, T.P, Zhang, F.F., Zhang, Y.H., Bi, X.W., 2010. Petrogenesis of late Triassic post-collisional basaltic rocks of the Lancangjiang tectonic zone, southwest China, and tectonic implications for the evolution of the eastern Paleotethys: geochronological and geochemical constraints. Lithos 119, 553–568.

Wang, Y.J., Zhao, G.C., Cawood, P.A., Fan, W.M., Peng, T.P., Sun, L.H., 2008. Geochemistry of Paleoproterozoic (~1770 Ma) mafic dikes from the Trans-North China Orogen and tectonic implications. Journal of Asian Earth Sciences 33, 61–77.

Wei, G.J., Liang, X.R., Li, X.H., Liu, Y., 2002. Precise measurement of Sr isotopic compositions of liquid and solid base using (LP) MC-ICP-MS. Geochimica 31 (3), 295–305.

Wonganan N, Caridroit M. 2005. Middle and Upper Devonian radiolarian faunas from Chiang Dao area, ChiangMai Province, northern Thailand. Micropaleontology 51(1), 39—57.

Wonganan, N., Caridroit, M., 2005. Middle and upper Devonian radiolarian fauna from Chiang Dao area, Chiang Mai Province, northern Thailand. Micropaleontology 51, 39–57.

Wonganan, N., Rarine, R., Caridroit, M., 2007. Mississippian (early Carboniferous) radiolarian biostratigraphy of northern Thailand (Chiang Dao area). Geobios 40, 875–888.

Wongwanich, T., Boucot, A.J., 2011. Devonian. In: Ridd, M.F., Barber, A.J., Crow, M.J., (eds.), The Geology of Thailand. Geological Society, London, pp. 71–136.

Xu, Y.G., Mei, H.J., Xu, J.F., Huang, X.L., Wang, Y.J., Chung, S.L., 2003. Origin of two differentiation trends in the Emeishan flood basalts. Chinese Science Bulletin 48, 390–394.

Yan, Q.S., Castillo, P., Shi, X.F., Wang, L.L., Liao, L., Ren, J.B., 2015. Geochemistry and petrogenesis of volcanic rocks from Daimao Seamount (South China Sea) and their tectonic implications. Lithos 218, 117–126.

Yang, W.Q., Qian, X., Feng, Q.L., Shen, S.Y., Chonglakmani, C., 2015. U-Pb geochronologic evidence for the evolution of Nan-Uttaradit suture zone in northern Thailand. Journal of Earth Science, in press.

Yin A., Harrison T.M., 2000. Geologic evolution of the Himalayan-Tibetan orogen. Annual Review of Earth and Planetary Sciences 28, 211–280.

Zhang, Y.Z., Wang, Y.J., Srithai, B., Phajuy, B., 2016. Petrogenesis for the Chiang Dao Permian high-iron basalt and its implication on the Paleotethyan Ocean in NW Thailand. Journal of Earth Science. doi: 10.1007/s12583-015-0646-4.

Zhong, D.L., 1998. The Paleotethys orogenic belt in west of Sichuan and Yunnan. Science Publishing House, Beijing, pp. 1–230 (in Chinese).

Figure captions

Fig. 1. (a) Tectonic sketch map of SE Asia showing major tectonic boundaries. (b) Tectonic subdivision in NW Thailand showing the Sibumasu block, Inthanon zone, Sukhothai zone and Indochina block from west to east, which are in turn separated by the Mae Yuam fault, the Chiang Rai fault and Nan suture zone, respectively.

Fig. 2. (a) Distribution of late Paleozoic volcanic rocks in Thailand (after Ridd et al., 2011). (b) Geological map in NW Thailand showing sampling locations. (c) Representative stratigraphic profiles at Chiang Dao and Fang showing seamount association (revised after Feng, 2002).

Fig. 3. Micrographs of the representative Group 1 (a, TG-2A; and b, TG-12L) and Group 2 (c, TG-4G; d, TG-14A_6) samples in NW Thailand.

Fig. 4. The $^{40}Ar/^{39}Ar$ age spectra of the basaltic sample (TG-4A) in NW Thailand. The length of bars reflects 1σ uncertainty. See Fig. 2b for locations of the sample.

Fig. 5. Plots of (a) Zr/Ti versus Nb/Y, (b) TiO_2 versus MgO and, (c) FeOt versus SiO_2 for the basaltic samples at the Chiang Mai area of NW Thailand. The fields of Emeishan basalts and Skaergaard Fenner basalts in (b-c) are from Xu et al. (2003) and Brooks et al. (1991), respectively.

Fig. 6. Harker diagram involving MgO versus (a) Al_2O_3, (b) SiO_2, (c) TiO_2, (d) CaO, (e) K_2O+Na_2O and (f) MnO for the Group 1 and 2 basalts in NW Thailand, respectively.

Fig. 7 MgO versus (a) Sc, (b) Co, (c) V, (d) Cr, (e) Ni, and Zr versus (f) Y, (g) Nb, (h) La, (i) Th and (j) Sr for the Group 1 and 2 basalts at the Chiang Mai area of NW

Thailand, respectively.

Fig. 8. The patterns of (a) the chondrite-normalized rare-earth elements, and (b) primitive mantle-normalized spidergram for the Group 1 and 2 basalts at the Chiang Mai area of NW Thailand, respectively. Chondrite- and primitive mantle-normalize values are from Sun and McDonough (1989). Data for OIB and E-MORB are after Sun and McDonough (1989).

Fig. 9. Plot of $\varepsilon_{Nd}(t)$ versus initial $^{87}Sr/^{86}Sr(t)$ for the representative samples from Group 1 and 2 at the Chiang Mai area of NW Thailand, respectively. Data for Hawaii OIB, Kenya, Samoa, Kergulen, Emeishan high-Ti and low-Ti basalts are from Xu et al. (2003) and Hart (1989).

Fig. 10. Plots of (a) Th and Ni, (b) Yb and La/Yb and (c) Yb and Tb/Yb for the Group 1 and 2 samples at the Chiang Mai area of NW Thailand, respectively.

Fig. 11. Plots of (a) La/Nb vs Nb/Th, (b) Zr/Y vs Nb/Y, (c) Th/Ta vs Tb/Ta, and (d) La/Sm vs Th/Yb for the Group 1 and 2 samples at the Chiang Mai area of NW Thailand, respectively. IAT: island-arc tholeiite; WPB: within-plate basalt; CAB: continental arc basalt; CFB: continental flood basalt; BAB: back-arc basin; MORB: mid-oceanic ridge basalt; E-MORB: enriched mid-oceanic-ridge basalt; N-MORB: normal mid-oceanic- ridge basalt; OIB: oceanic-island basalt; OIT: oceanic-island tholeiite; WPAB: within- plate alkali basalt.

Fig. 12. (a) Zr/Nb vs Ce/Y and (b) La/Sm vs Sm/Yb for Group 1 and 2 at the Chiang Mai area of NW Thailand, respectively.

Fig. 13. Late Paleozoic paleography in NW Thailand showing the trench-arc

system. Form west to east, the spatial pattern is characterized by the Sibumasu block, Inthanon zone, Sukhothai zone, Nan back-arc zone and Indochina block.

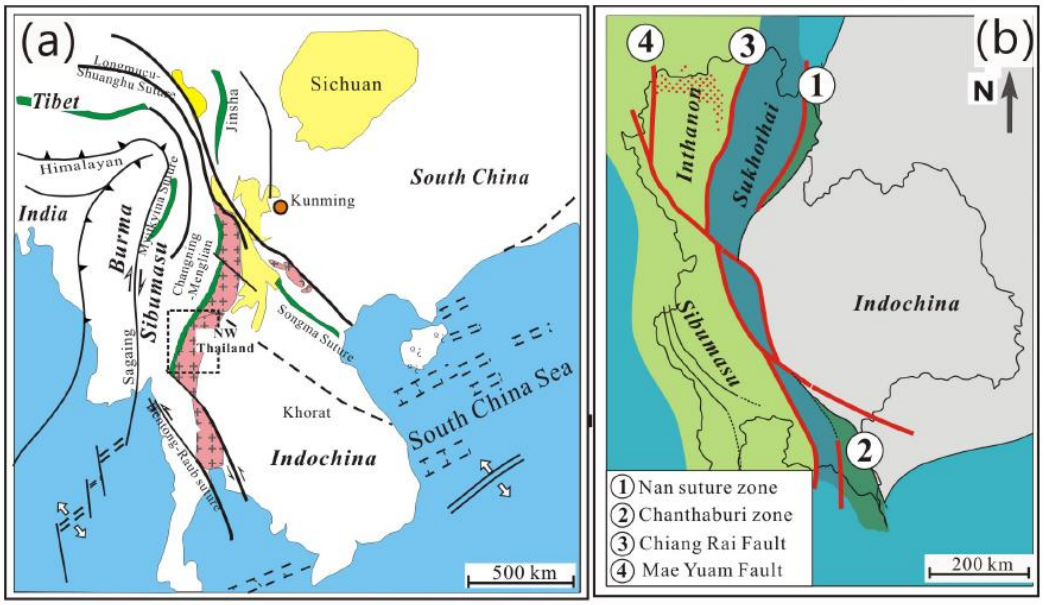

Figure 1 Y-J Wang & coauthors

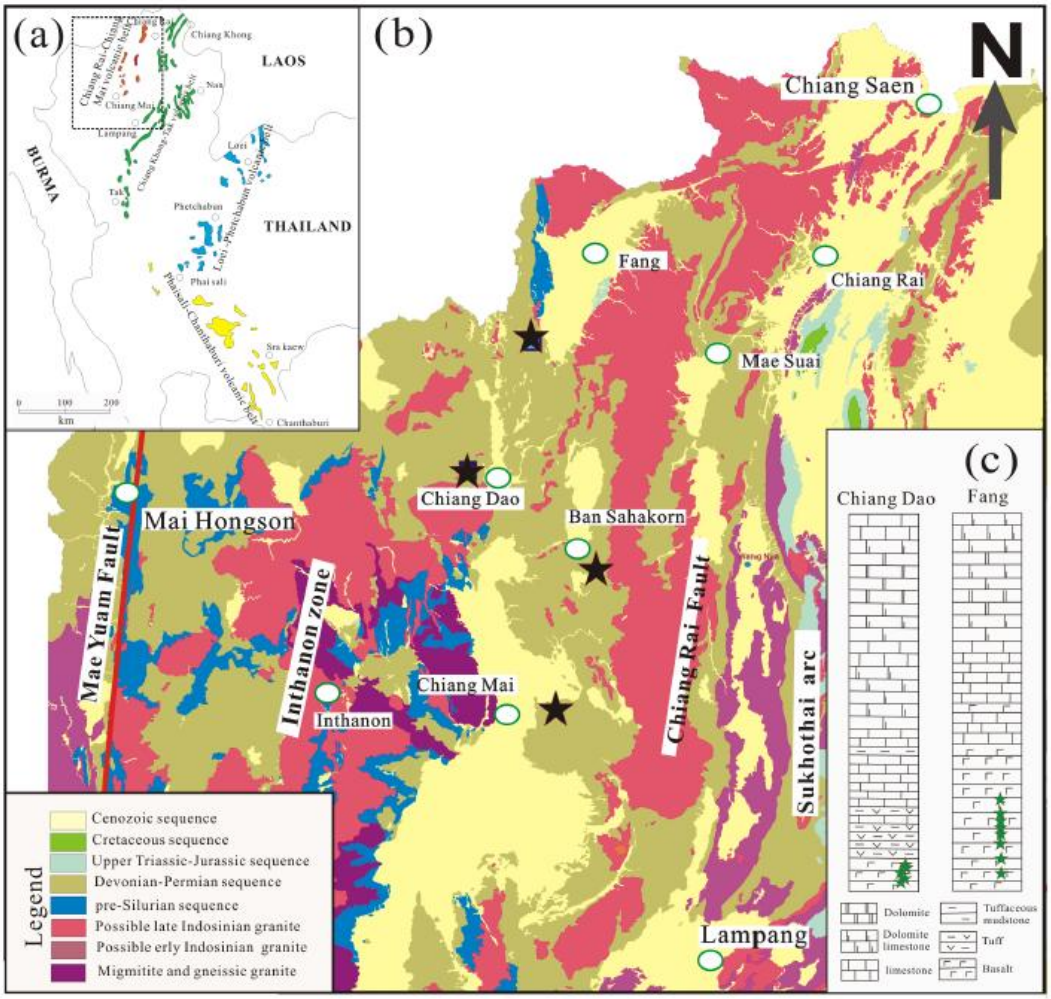

Figure 2 Y-J Wang & coauthors

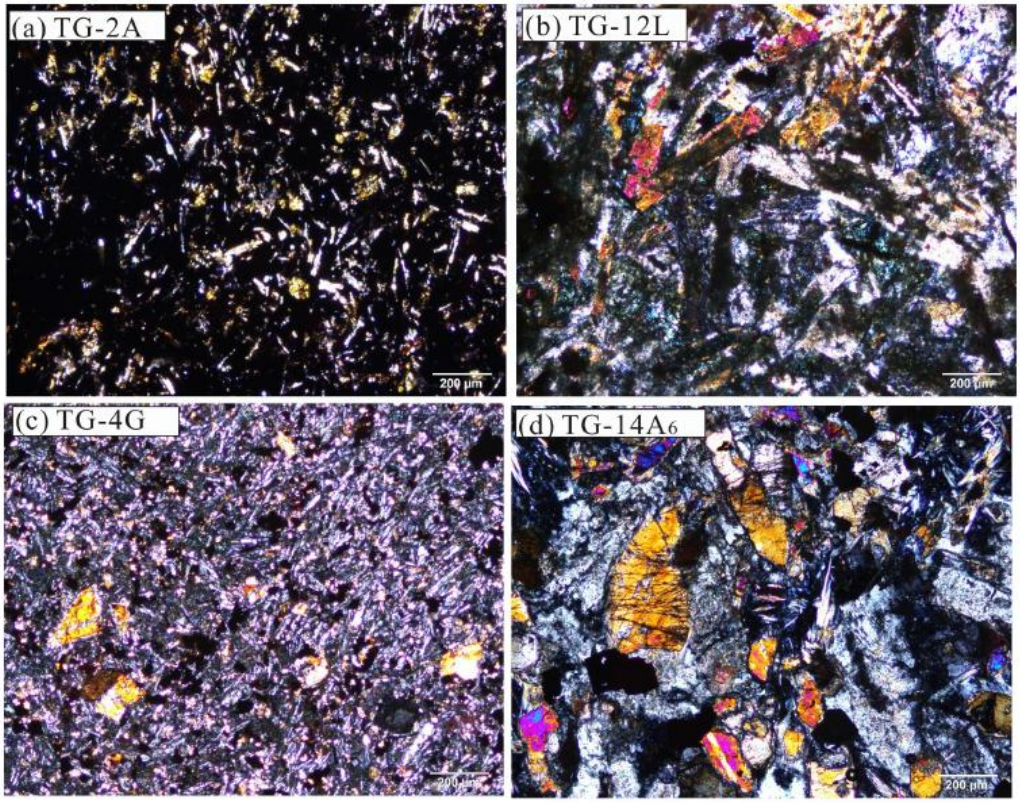

Fig. 3 Y-J Wang & coauthors

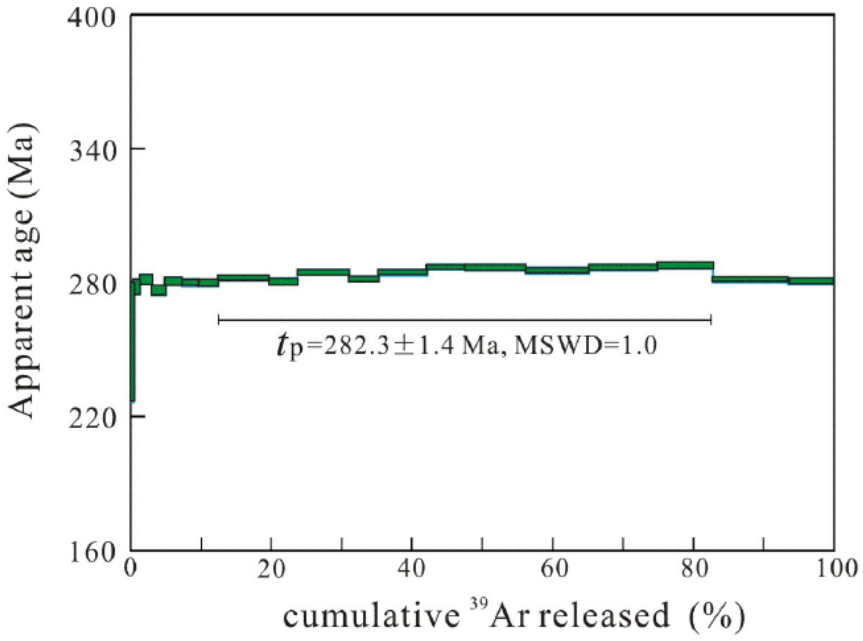

Fig. 4 Y-J Wang and coauthors

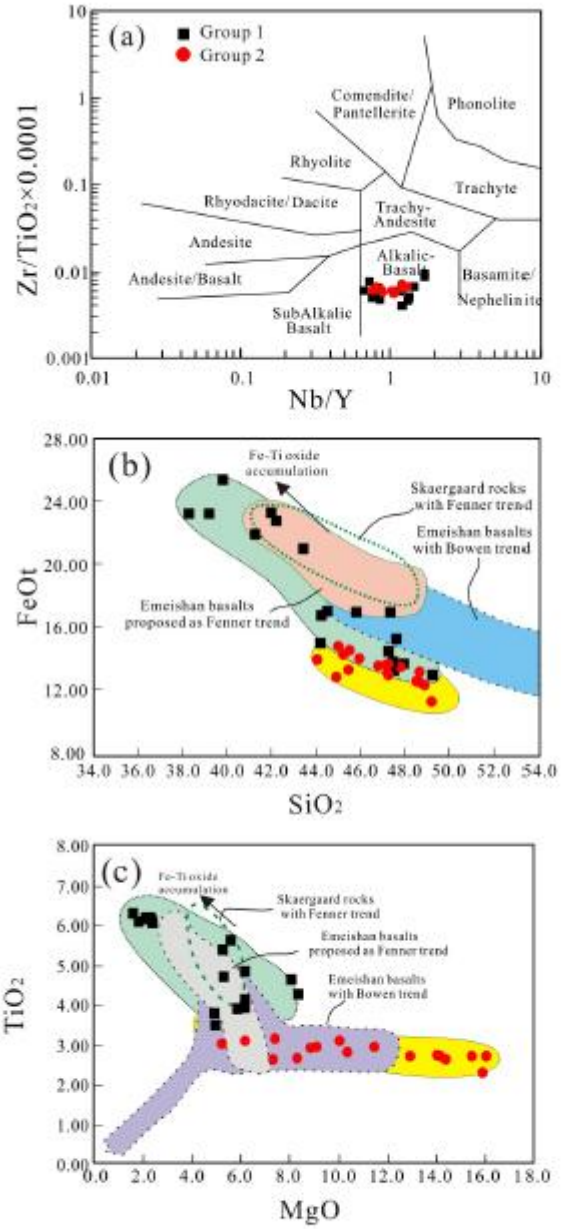

Fig. 5 Y-J Wang & coauthors

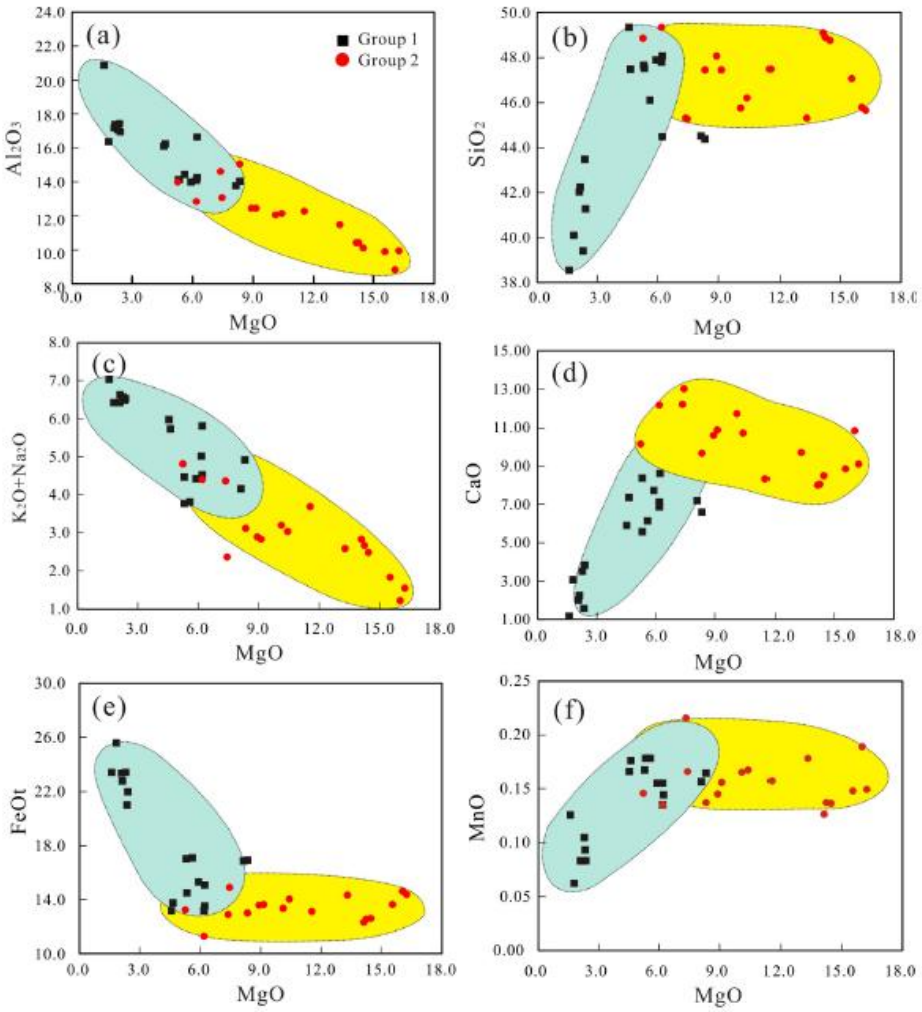

Fig. 6 Y-J Wang and coauthors

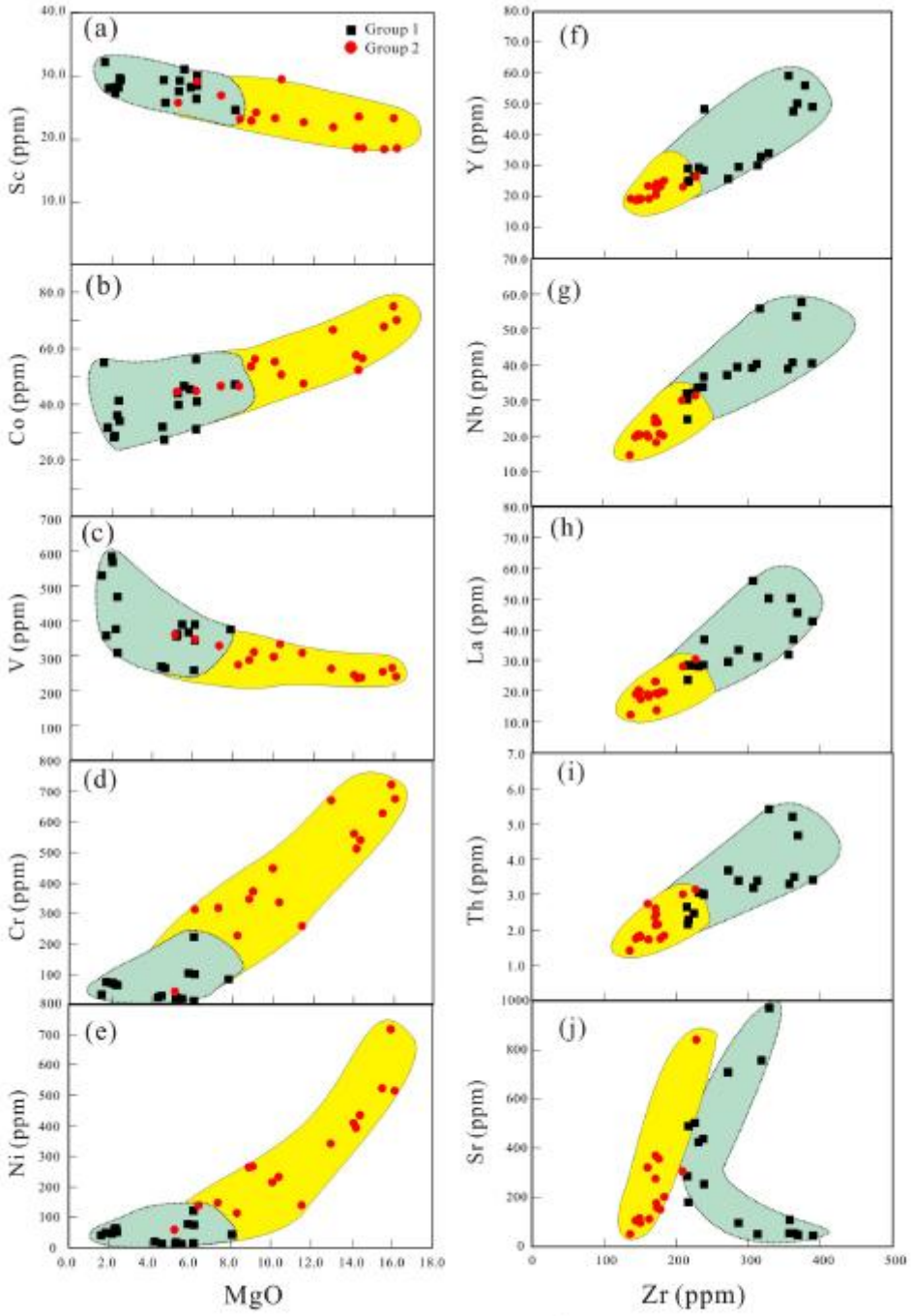

Fig. 7 Y-J Wang & coauthors

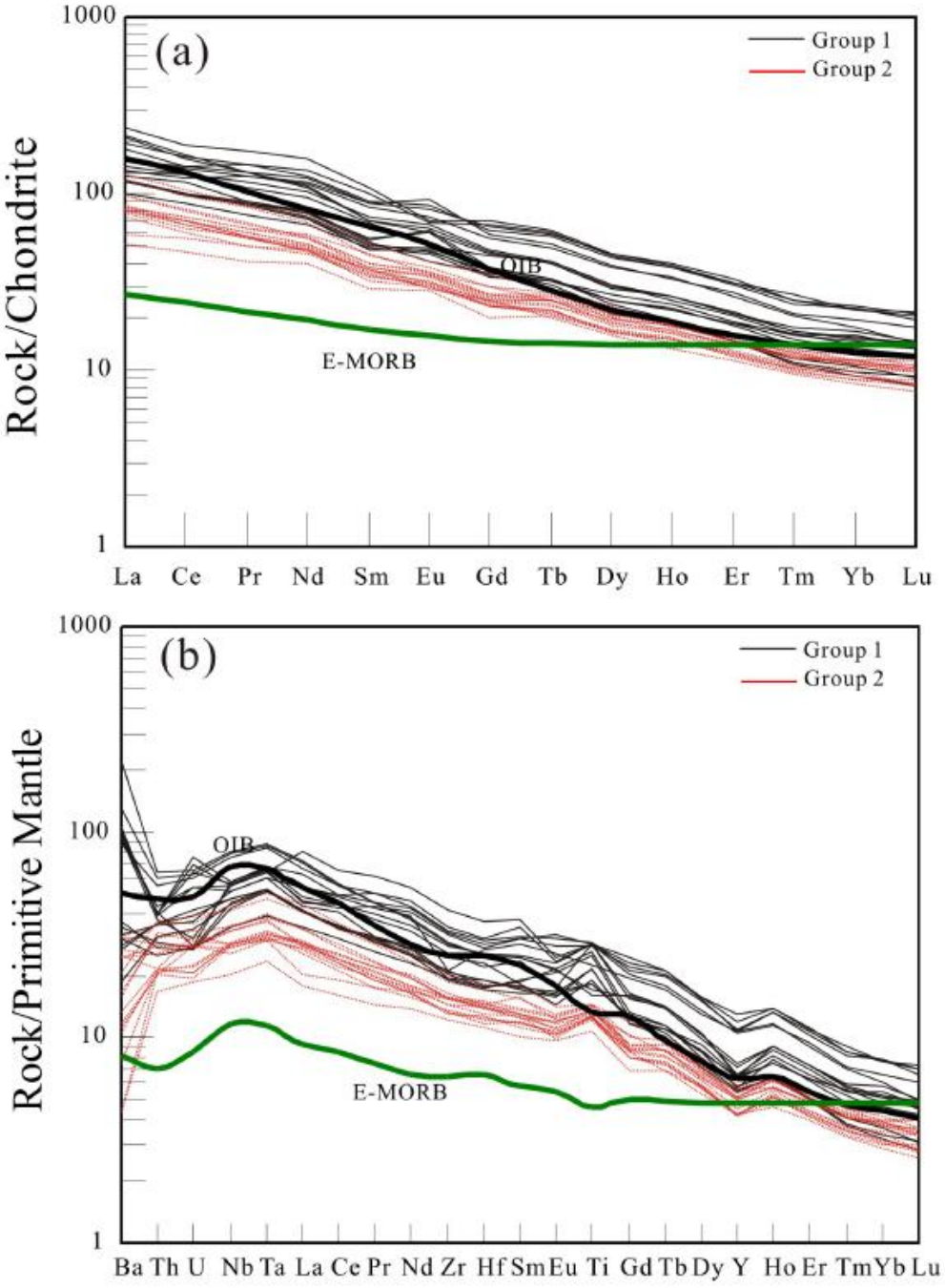

Fig. 8 Y-J Wang & coauthors

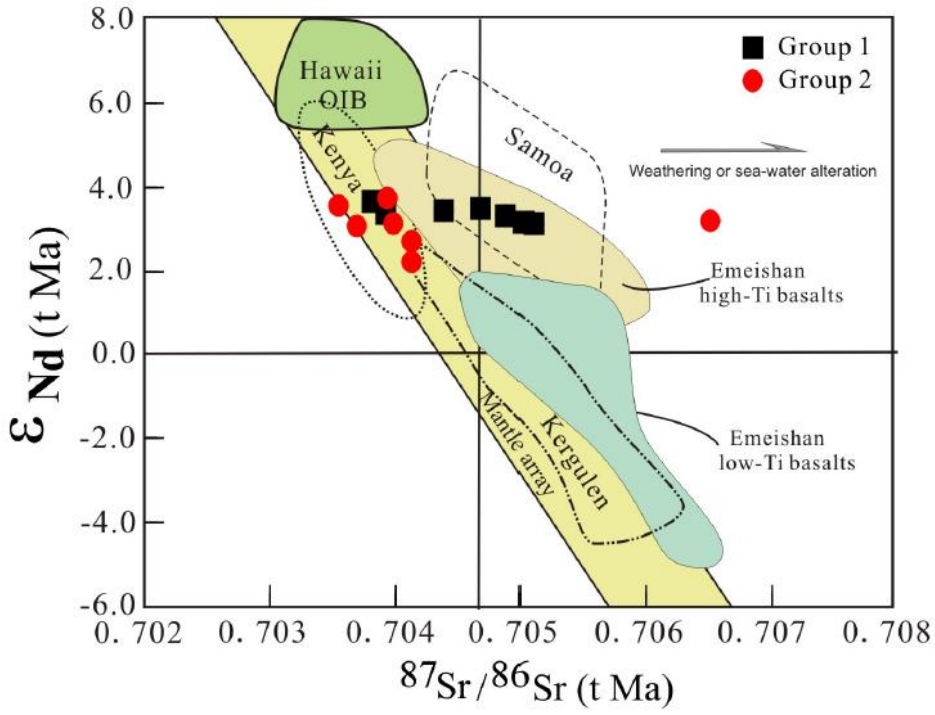

Fig. 9 Y-J Wang & coauthors

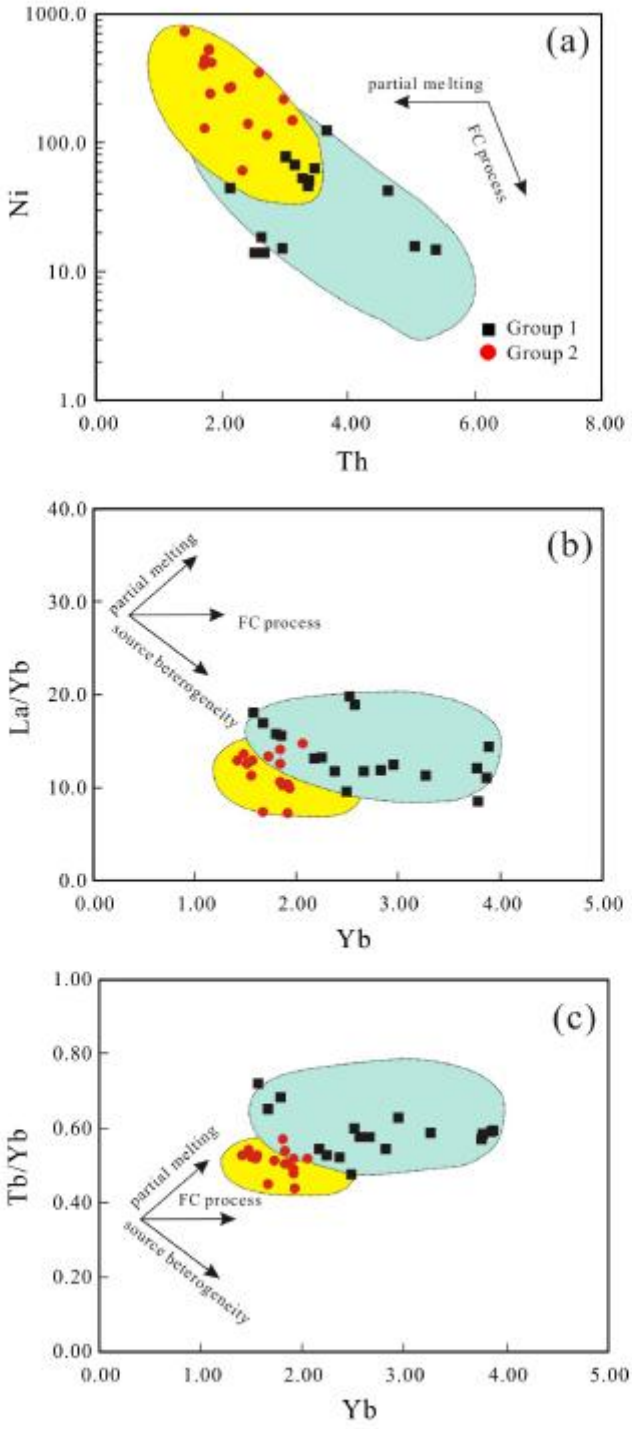

Fig. 10 Y-J Wang and coauthors

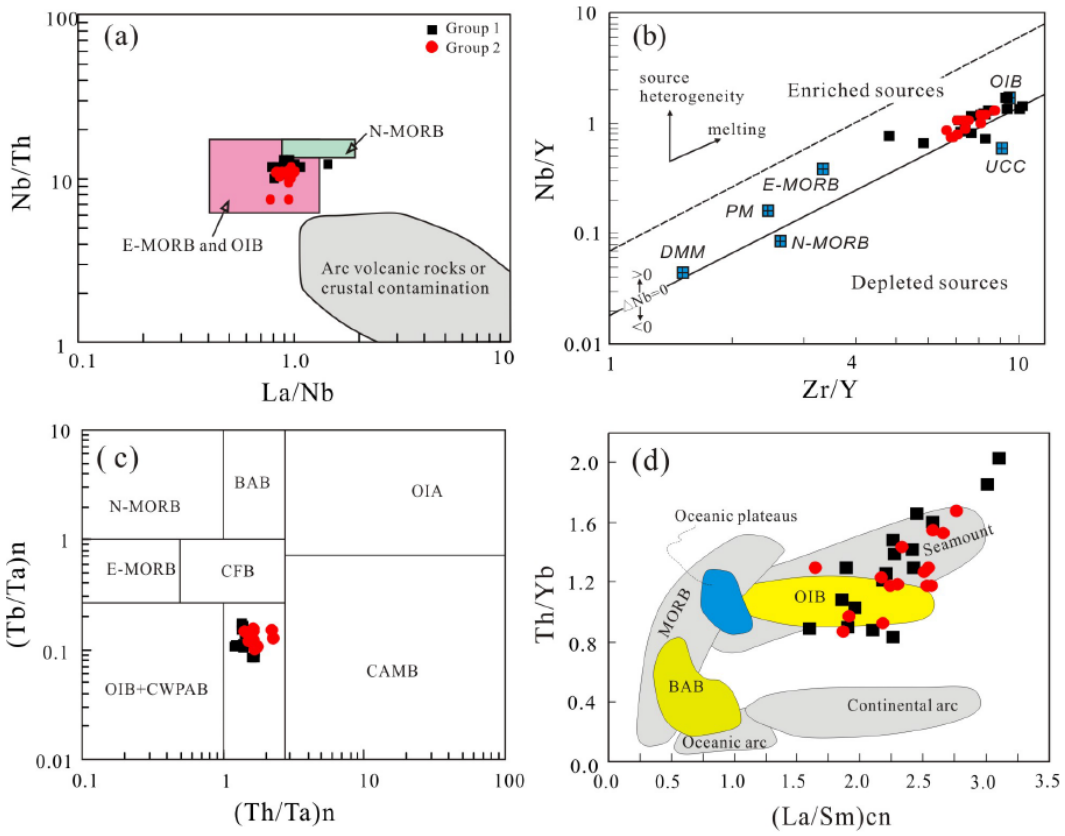

Fig. 11 Y-J Wang & coauthors

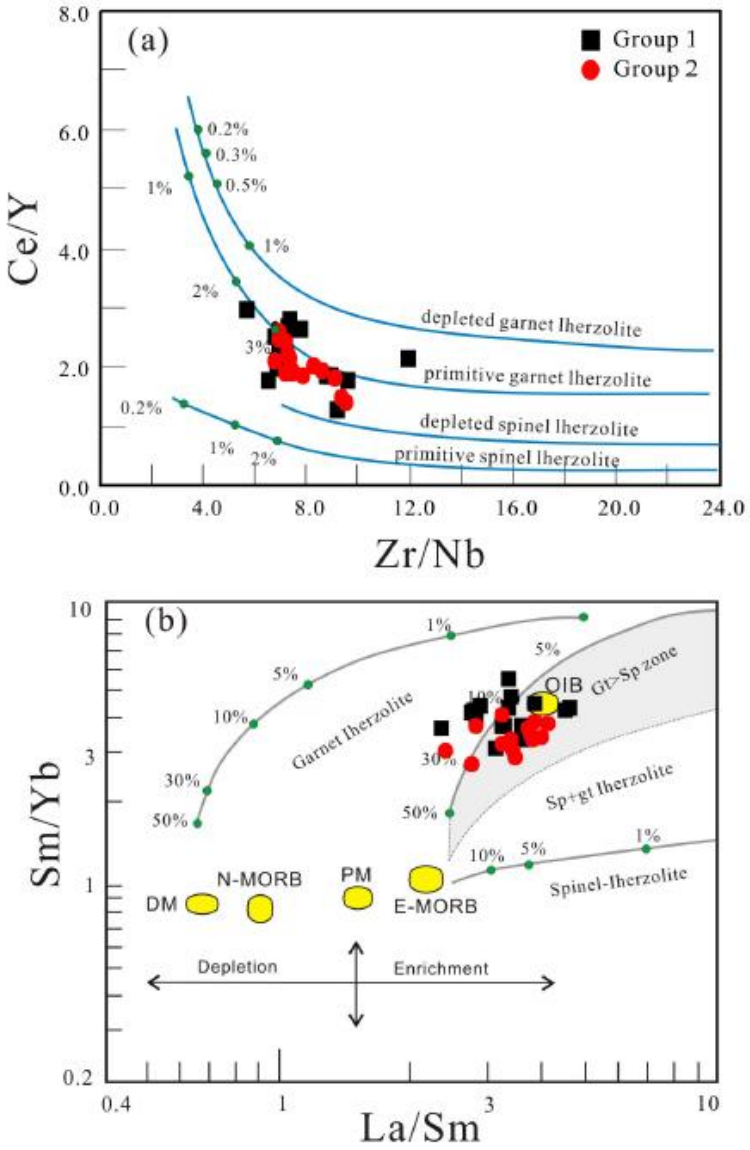

Fig. 12 Y-J Wang & coauthors

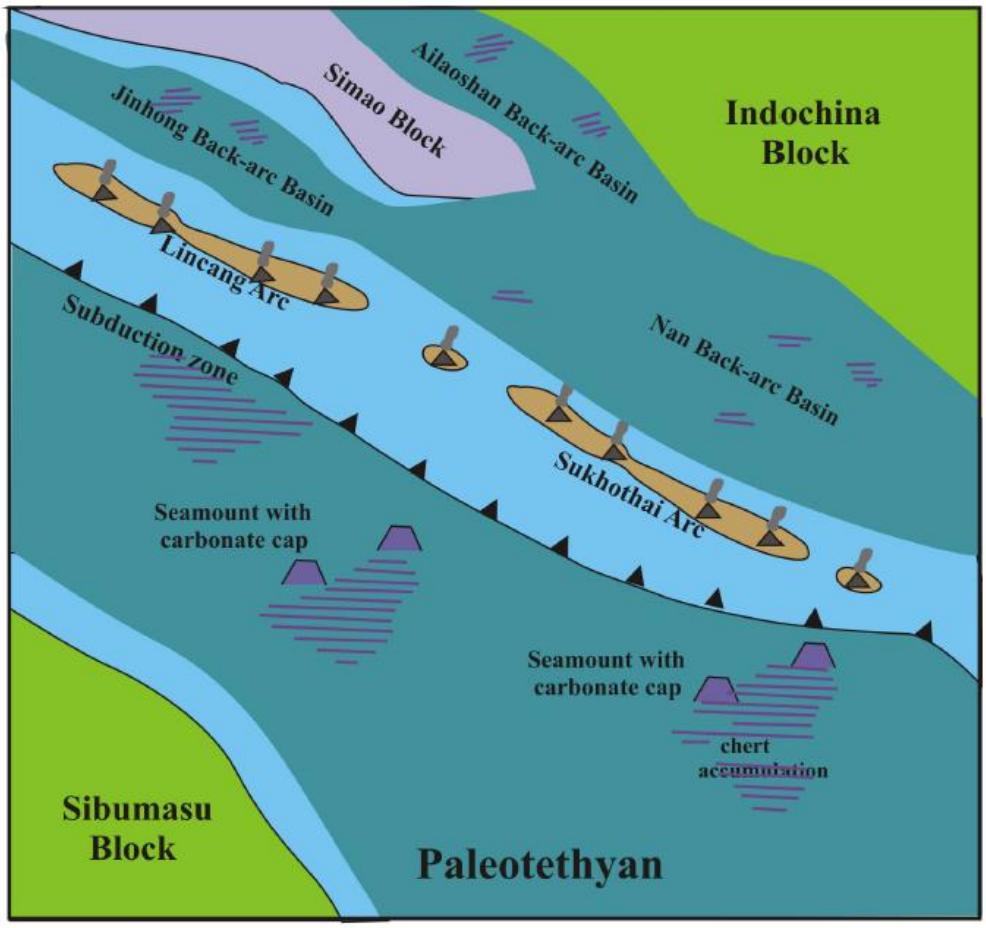

Fig. 13 Y-J Wang & coauthors

Highlights

► The Chiang Mai basaltic rocks are characterized by high-Fe basalts with distinct differentiation trends.

► These basalts in NW Thailand originated from an OIB-like source in the Paleotethyan intra-oceanic seamount setting.

► The Inthanon zone defines the Paleotethyan main suture with the Chiang Rai Fault for the easternmost boundary.